IMMUNOLOGY

Mitofusin 2 Inhibits Mitochondrial Antiviral Signaling

Kai Yasukawa,[1] Hiroyuki Oshiumi,[2] Makoto Takeda,[3] Naotada Ishihara,[4] Yusuke Yanagi,[3] Tsukasa Seya,[2] Shun-ichiro Kawabata,[1] Takumi Koshiba[1]*

(Published 18 August 2009; Volume 2 Issue 84 ra47)

The innate immune response to viral infection involves the activation of multiple signaling steps that culminate in the production of type I interferons (IFNs). Mitochondrial antiviral signaling (MAVS), a mitochondrial outer membrane adaptor protein, plays an important role in this process. Here, we report that mitofusin 2 (Mfn2), a mediator of mitochondrial fusion, interacts with MAVS to modulate antiviral immunity. Overexpression of Mfn2 resulted in the inhibition of retinoic acid–inducible gene I (RIG-I) and melanoma differentiation–associated gene 5 (MDA-5), two cytosolic sensors of viral RNA, as well as of MAVS-mediated activation of the transcription factors interferon regulatory factor 3 (IRF-3) and nuclear factor κB (NF-κB). In contrast, loss of endogenous Mfn2 enhanced virus-induced production of IFN-β and thereby decreased viral replication. Structure-function analysis revealed that Mfn2 interacted with the carboxyl-terminal region of MAVS through a heptad repeat region, providing a structural perspective on the regulation of the mitochondrial antiviral response. Our results suggest that Mfn2 acts as an inhibitor of antiviral signaling, a function that may be distinct from its role in mitochondrial dynamics.

INTRODUCTION

Innate immunity is an essential and ubiquitous system that defends organisms from infectious pathogens. Initiation of the innate immune response is typically triggered by the recognition of broadly conserved elements of the invading pathogen known as pathogen-associated molecular patterns (PAMPs). The recognition of PAMPs by germline-encoded pattern recognition receptors ultimately activates intracellular signaling cascades that result in the clearance and killing of infectious microbes (*1*, *2*). Viral infection of host cells is detected by the cell's recognition of PAMPs such as double-stranded RNA (dsRNA), which initiates two distinct signaling pathways (*3*). The first, mediated by endosomal Toll-like receptor 3, recognizes viral dsRNA that enters the cell by endocytosis, whereas the second pathway detects cytoplasmic, virus-derived dsRNA through the involvement of two RNA helicases, retinoic acid–inducible gene I (RIG-I) and melanoma differentiation–associated gene 5 (MDA-5) (*3*). Although these two pathways differ with respect to their initiating stimuli and downstream effectors, they converge at the point of transcriptional activation, resulting in the rapid production of type I interferons (IFN-α and IFN-β) and other cytokines that promote the subsequent development of adaptive antiviral immunity (*4*, *5*).

Mitochondria, in addition to serving as the powerhouses of eukaryotic cells, are well characterized as crucial players in numerous cellular processes, including apoptosis (*6*), aging (*7*), and calcium homeostasis (*8*). Other studies, however, have revealed that mitochondria also play a fundamental role in antiviral immunity in mammals (*9*–*13*). Mitochondrial antiviral immunity depends on both the upstream activation of the RIG-I or MDA-5 pathway and the participation of mitochondrial antiviral signaling protein [MAVS (*9*), also known as IPS-1 (*14*), VISA (*15*), and Cardif (*16*)], a mitochondrial outer membrane protein that is a member of the caspase activation and recruitment domain (CARD) family. Cellular deficiency in MAVS abrogates the production of type I IFNs and prevents the activation of the transcription factors interferon regulatory factor 3 (IRF-3) and nuclear factor κB (NF-κB) after viral infection (*17*, *18*), thus underscoring the importance of the linkage between antiviral immunity and mitochondria. Although several cytoplasmic proteins have been functionally linked to the MAVS-dependent antiviral signaling pathway (*3*), the importance of other mitochondrial integral membrane proteins that potentially cooperate with MAVS has remained unclear. Here, we describe our findings that mitofusin 2 (Mfn2), a mediator of mitochondrial fusion, negatively regulates antiviral signaling through MAVS.

[1]Department of Biology, Faculty of Sciences, Kyushu University, 6-10-1 Hakozaki, Higashi-ku, Fukuoka 812-8581, Japan. [2]Department of Microbiology and Immunology, Graduate School of Medicine, Hokkaido University, Kita-ku, Sapporo 060-8638, Japan. [3]Department of Virology, Faculty of Medicine, Kyushu University, Higashi-ku, Fukuoka 812-8582, Japan. [4]Department of Physiology and Cell Biology, Tokyo Medical and Dental University, Tokyo 113-8519, Japan. *To whom correspondence should be addressed. E-mail: koshiba@kyudai.jp

RESULTS

MAVS assembles into a high molecular mass complex on mitochondria

We reasoned that additional mitochondrial membrane proteins could functionally and physically interact with MAVS to regulate mitochondrial antiviral immunity. To test this hypothesis, we examined the molecular mass of endogenous MAVS by size exclusion chromatography. Despite having a predicted molecular mass of 56 kD, endogenous MAVS extracted from the mitochondrial fraction of human embryonic kidney (HEK) 293 cells eluted in a high molecular mass fraction that corresponded to ~600 kD at physiological pH (pH 7.2) (Fig. 1A). A similar result was obtained with N-terminal Myc-tagged MAVS that was stably expressed in HEK 293 cells (Fig. 1A). To verify that the observed molecular mass of the MAVS complex was not due to nonspecific aggregation under these experimental conditions, we analyzed Fis1, a C-terminal tail–anchored mitochondrial outer membrane protein that similarly forms higher-order complexes. Fis1 derived from mitochondrial extracts of HEK 293 cells eluted at a position corresponding to less than 230 kD (Fig. 1A), consistent with previous studies (*19*). These findings indicated that MAVS ordinarily forms a stable higher-order complex on the outer mitochondrial membrane, and they raised the possibility that unidentified mitochondrial components of this complex could be relevant to the mitochondrial antiviral response.

MAVS associates with the mitochondrial outer membrane guanosine triphosphatase, Mfn2

We next attempted to determine whether MAVS associated with previously unidentified cellular components by analyzing immunoprecipitated samples derived from HEK 293 cells stably expressing Myc-tagged MAVS. Analysis of samples immunoprecipitated with an antibody against the Myc tag by liquid chromatography with tandem mass spectrometry (LC/MS/MS) identified several mitochondrial proteins (table S1). Plasmids encoding these proteins were individually coexpressed with a plasmid encoding MAVS by transient transfection of HEK 293 cells. Of these candidates, the mitochondrial outer membrane guanosine triphosphatase (GTPase) Mfn2, which mediates mitochondrial fusion (*20*), coimmunoprecipitated with MAVS (Fig. 1B). In addition, we confirmed that MAVS coimmunoprecipitated with endogenous Mfn2 in HEK 293 cells (Fig. 1C). The interaction between endogenous Mfn2 and MAVS was also observed in mouse embryonic fibroblasts (MEFs) (fig. S1). Consistent with this observation, MAVS and Mfn2 mRNAs showed similar expression patterns in human tissues (*15*, *21*), and the colocalization of both endogenous proteins to mitochondria was confirmed in MEFs by fluorescence microscopy (Fig. 1D). Although Mfn2 is a large transmembrane GTPase that is well known for mediating mitochondrial fusion, it has additionally been reported to act as an endoplasmic reticulum (ER)–mitochondrion tether (*22*), as a suppressor of cellular proliferation (*23*) and as a pathogenic factor in inherited peripheral neuropathy (*24*).

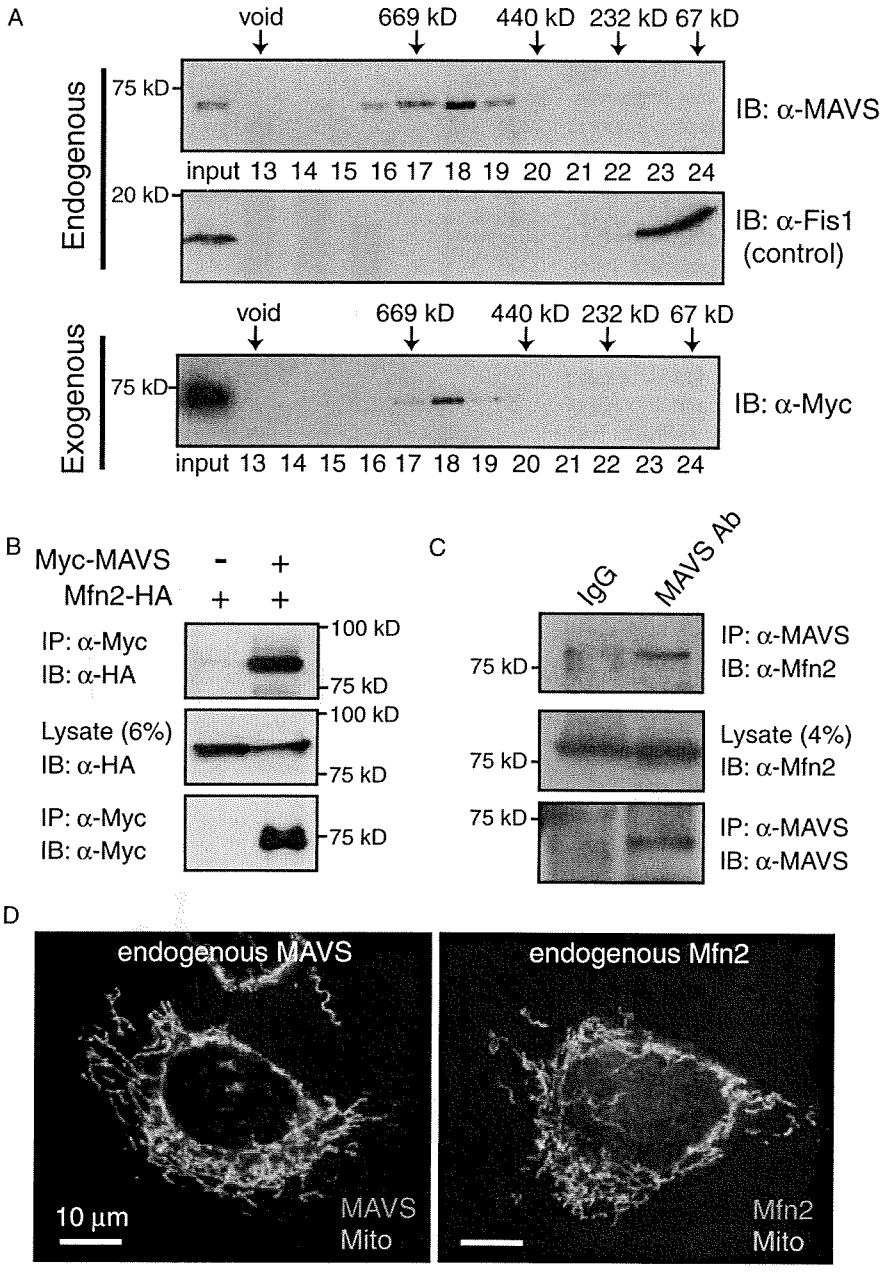

Fig. 1. MAVS is a component of a supramolecular protein complex. (A) Size exclusion chromatography (Superdex-200 HR-10/30 column) of endogenous and exogenous MAVS at pH 7.2. The positions corresponding to the elution of standard markers of molecular mass and the void volume are indicated. Fractions (numbered) were analyzed by Western blotting with a polyclonal antibody against hMAVS (to detect endogenous protein) or the 9E10 monoclonal antibody against Myc (to detect tagged protein), as well as with a polyclonal antibody against Fis1 for the control analysis. (B) HEK 293 cells were cotransfected with combinations of plasmids encoding HA-tagged Mfn2 and Myc-tagged MAVS, as indicated. Western blots of samples immunoprecipitated (IP) with an antibody against Myc or postnuclear cell lysates (lysate; 6% of the input) were analyzed by immunoblotting (IB) with either the monoclonal antibody HA.11 against HA or the monoclonal antibody 9E10 against Myc. (C) Interaction of endogenous Mfn2 with MAVS. Lysates of HEK 293 cells were subjected to immunoprecipitation with anti-MAVS polyclonal antibody or control IgG followed by the analysis of Western blots with an antibody against Mfn2. Lysate, 4% of the input. In (A) to (C), α denotes "anti-". (D) Endogenous MAVS (red) and Mfn2 (red) colocalize with mitochondria in MEFs. Mitochondria were stained with a monoclonal antibody against mtHsp70 (green). Scale bar, 10 μm.

Mfn2 inhibits MAVS-mediated activation of IRF-3 and NF-κB

Having identified Mfn2 as a component of the MAVS complex, we investigated whether this protein modulated MAVS-mediated activation of IFN-β and NF-κB reporter constructs. Although MAVS potently activated both IFN-β and NF-κB luciferase–based reporters, as seen previously (*9*, *14–16*), Mfn2 alone failed to activate either reporter construct (Fig. 2A). However, coexpression of Mfn2, but not the unrelated mitochondrial outer membrane protein Fis1, with MAVS was sufficient to inhibit MAVS-dependent activation of IFN-β and NF-κB reporters in a dose-dependent manner (Fig. 2B). This inhibitory activity was not observed with the Mfn2 homolog, Mfn1, despite the ~60% sequence identity between the two proteins (*21*), which indicated that the observed inhibitory activity toward MAVS-mediated signaling was specific to Mfn2 (Fig. 2C). The inhibition that resulted from the increased abundance of Mfn2 was not attributable to general mitochondrial dysfunction because most cells that contained both overexpressed MAVS and Mfn2 exhibited normal tubular mitochondrial morphology that was indistinguishable from that of untransfected cells (Fig. 2D).

Because MAVS-dependent antiviral signaling is potentiated by the recognition of viral dsRNA by the cytoplasmic RNA helicases RIG-I and MDA-5, we sought to determine the effect of Mfn2 on the ability of these sensor helicases and dsRNA to induce downstream activation of IRF-3 and the IFN-β reporter. Overexpression of the N-terminal CARD domains of RIG-I [designated as RIG-I(1–250) in this study] induces a robust intracellular antiviral response (*25*). Mfn2 dramatically reduced the ability of RIG-I(1–250) to activate the IFN-β reporter in a dose-dependent manner (Fig. 3A) and similarly reduced the production of endogenous IFN-β protein

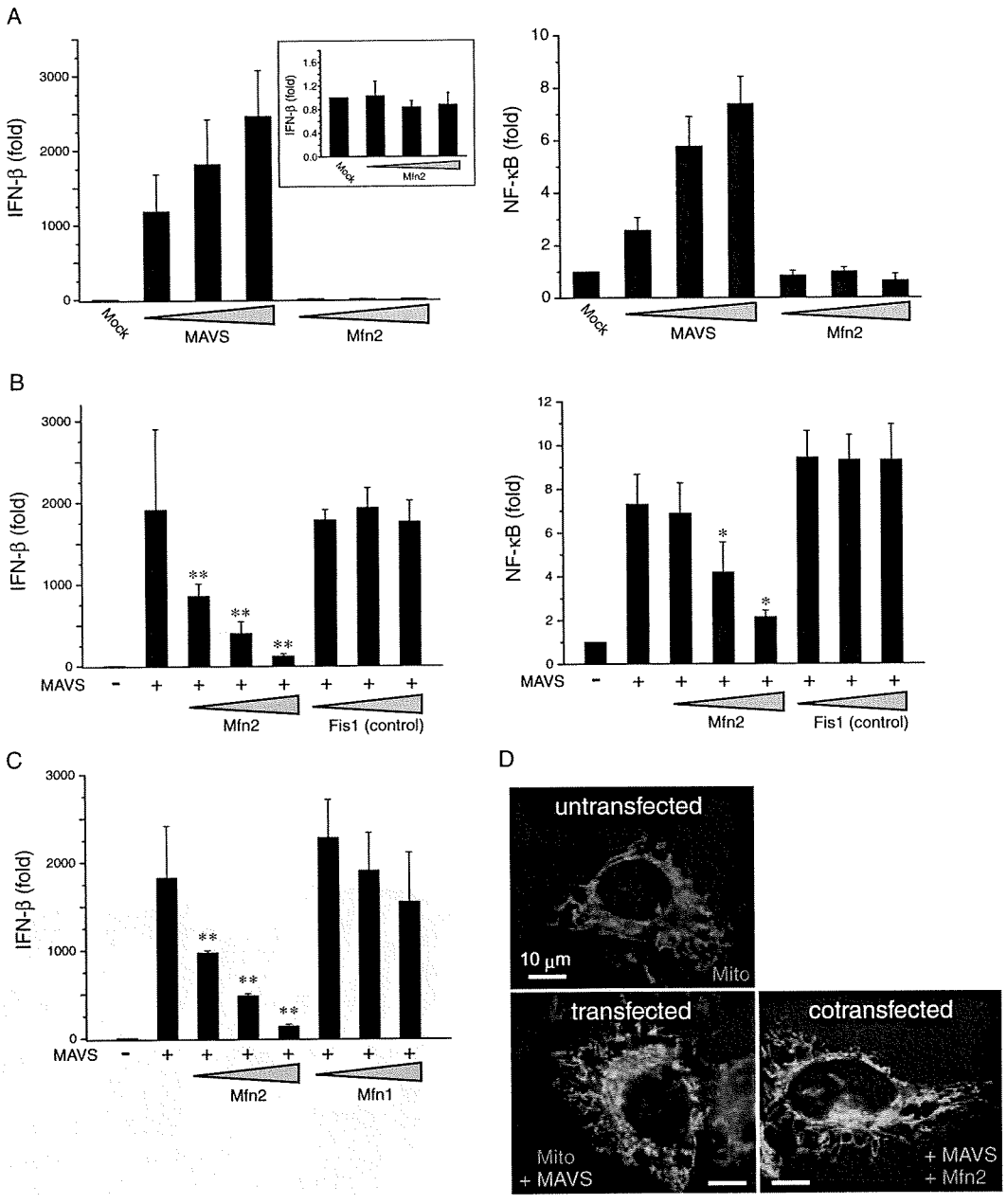

Fig. 2. Mfn2 inhibits MAVS-mediated activation of IFN-β and NF-κB reporters. (A) HEK 293 cells were transfected with empty vector (Mock) or increasing amounts (20, 50, and 100 ng) of plasmids encoding MAVS (positive control) or Mfn2 and with either IFN-β (left panel) or NF-κB (right panel) luciferase reporter plasmids. Inset: a magnified scale of Mfn2 result. (B) HEK 293 cells were cotransfected with 50 ng of a plasmid encoding MAVS and increasing amounts (20, 50, and 100 ng) of plasmids encoding Mfn2 or Fis1 (negative control) together with the same reporter plasmids used in (A). (C) The Mfn2 homolog, Mfn1, does not inhibit MAVS-mediated activation of IFN-β reporter. The resulting IFN-β reporter activity was determined as above. All data shown represent mean values ± SD (n = 3 experiments). *$P < 0.05$; **$P < 0.01$. (D) Immunofluorescence microscopy of untransfected HeLa cells, HeLa cells transfected with a plasmid encoding MAVS, or HeLa cells cotransfected with plasmids encoding MAVS and Mfn2. Cells were visualized with MAVS [enhanced green fluorescent protein; green], Mfn2 (Alex Fluor 568; red), and mitochondria (red fluorescent protein; red). Scale bar, 10 μm.

as determined by enzyme-linked immunosorbent assay (ELISA) (Fig. 3B). We additionally examined the activation of endogenous IRF-3 by performing gel-shift assays. Expression of RIG-I(1–250) promoted the hallmarks of IRF-3 activation, namely, its dimerization and phosphorylation (Fig. 3C), both of which were impaired by Mfn2 in a dose-dependent manner (Fig. 3C).

Overexpression of Mfn2 additionally abrogated the effect of MDA-5 in a dose-dependent manner (Fig. 3D). MDA-5 is the intracellular receptor for poly(I:C), a synthetic analog of viral double-stranded RNA (*26*, *27*). Consistent with previous findings, the delivery of poly(I:C) into HEK 293 cells by transient transfection stimulated the IFN-β response, which was suppressed by Mfn2 (Fig. 3E). In contrast, Mfn2 did not impair the IFN-β response to extracellular poly(I:C) (Fig. 3E). Taken together, these results indicate that Mfn2 acted as a negative regulator of RIG-I–, MDA-5–, and dsRNA-dependent antiviral signaling through MAVS and suggested that the association of MAVS and Mfn2 might underlie this inhibition.

Loss of endogenous Mfn2 results in enhanced RIG-I– and MDA-5–induced antiviral responses

The previous experiments showed that Mfn2 suppressed MAVS-dependent signaling. We therefore attempted to determine, through an RNA interference

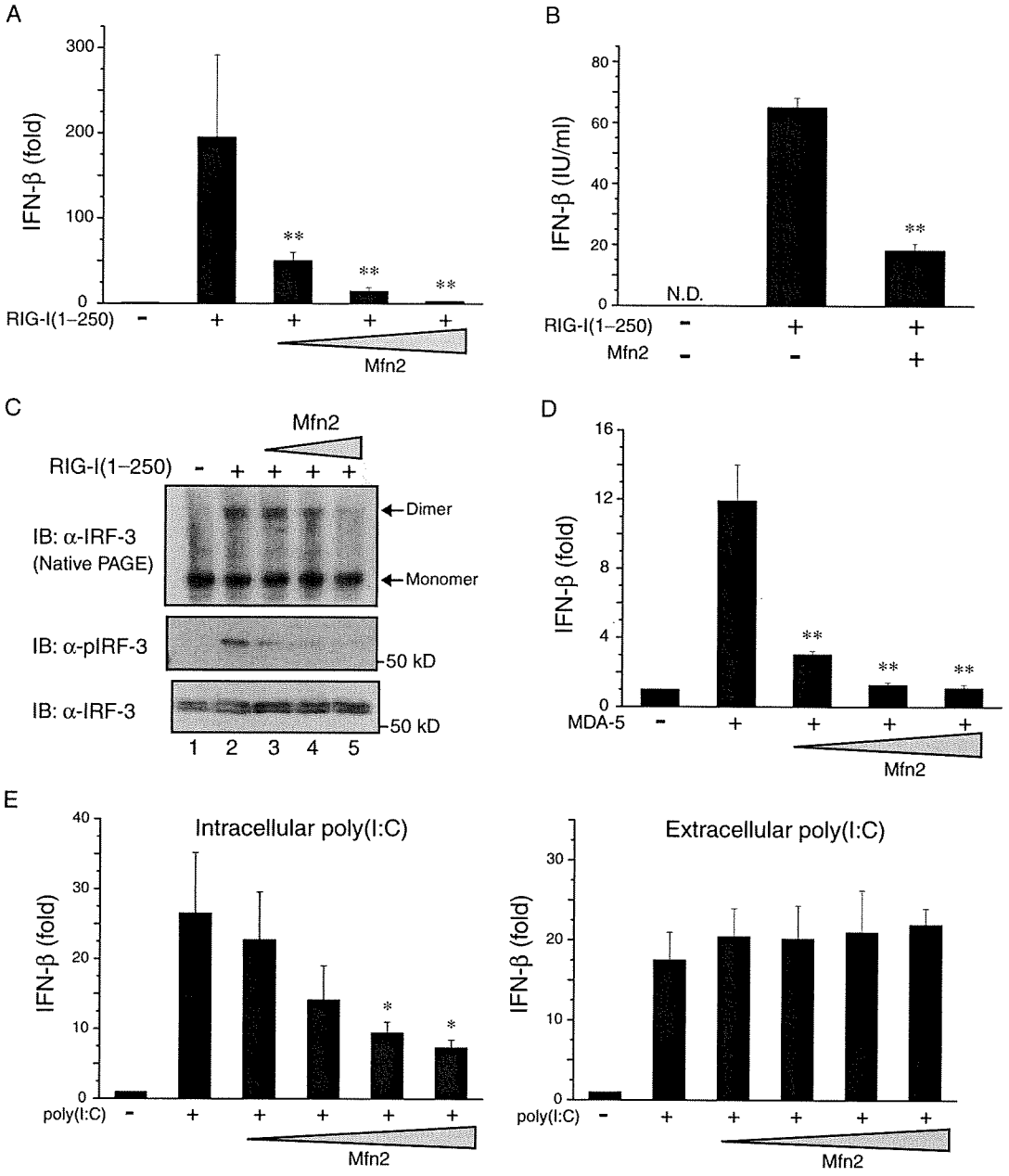

Fig. 3. Mfn2 suppresses IFN-β signaling mediated by RIG-I and MDA-5. (A) HEK 293 cells were cotransfected with 50 ng of plasmid encoding RIG-I(1–250) with increasing amounts (20, 50, and 100 ng) of a plasmid encoding Mfn2 together with the luciferase reporter plasmid p125luc. Transfected cells were analyzed 24 hours later for IFN-β–dependent luciferase activity. (B) HEK 293 cells were cotransfected with 200 ng of plasmid encoding RIG-I(1–250) and 200 ng of a plasmid encoding either pcDNA3.1 (negative) or Mfn2. Culture supernatants were harvested 24 hours after transfection and analyzed by ELISA to measure the production of IFN-β. (C) HEK 293 cells were cotransfected with 300 ng of a plasmid encoding RIG-I(1–250) and increasing amounts (100, 300, and 500 ng) of the plasmid encoding Mfn2. Cell lysates were resolved by electrophoresis under native (top panel) or denaturing conditions (middle and bottom panels) and then analyzed by Western blotting with the indicated antibodies. (D) Experiments were performed similarly to those in (A), except that the plasmid encoding MDA-5 was used in the transfections instead of the plasmid encoding RIG-I(1–250). (E) HEK 293 cells were transfected with various amounts (20, 50, 100, and 200 ng) of the plasmid encoding Mfn2 and were either cotransfected with poly(I:C) (left panel) or treated extracellularly with poly(I:C) (right panel). The resulting IFN-β reporter activity was determined as described earlier. All data shown represent mean values ± SD (n = 3 experiments). *P < 0.05; **P < 0.01.

approach, whether endogenous Mfn2 was responsible for modulating the MAVS-dependent transcriptional activation of the gene encoding IFN-β. Consistent with our previous findings, HEK 293 cells that had been treated with Mfn2-specific small interfering RNA (siRNA), which efficiently knocked down the amount of endogenous Mfn2 protein by greater than 90% (Fig. 4, A and B), exhibited enhanced induction of the IFN-β reporter construct in response to RIG-I(1–250) relative to that of control siRNA–transfected cells (Fig. 4B). Moreover, reintroduction of Myc-tagged Mfn2 into HEK 293 cells that had been treated with Mfn2-specific siRNA restored the suppressive effect on RIG-I(1–250)–dependent induction of the IFN-β reporter (Fig. 4C). HEK 293 cells also exhibited a differential response to an increased abundance of MAVS when treated with the Mfn2-specific siRNA, with increased activation of the IFN-β reporter and production of endogenous IFN-β relative to that of cells treated with the control siRNA (fig. S2, A and B). Knockdown of endogenous Mfn2 by siRNA similarly enhanced the activation of the IFN-β reporter and the production of IFN-β

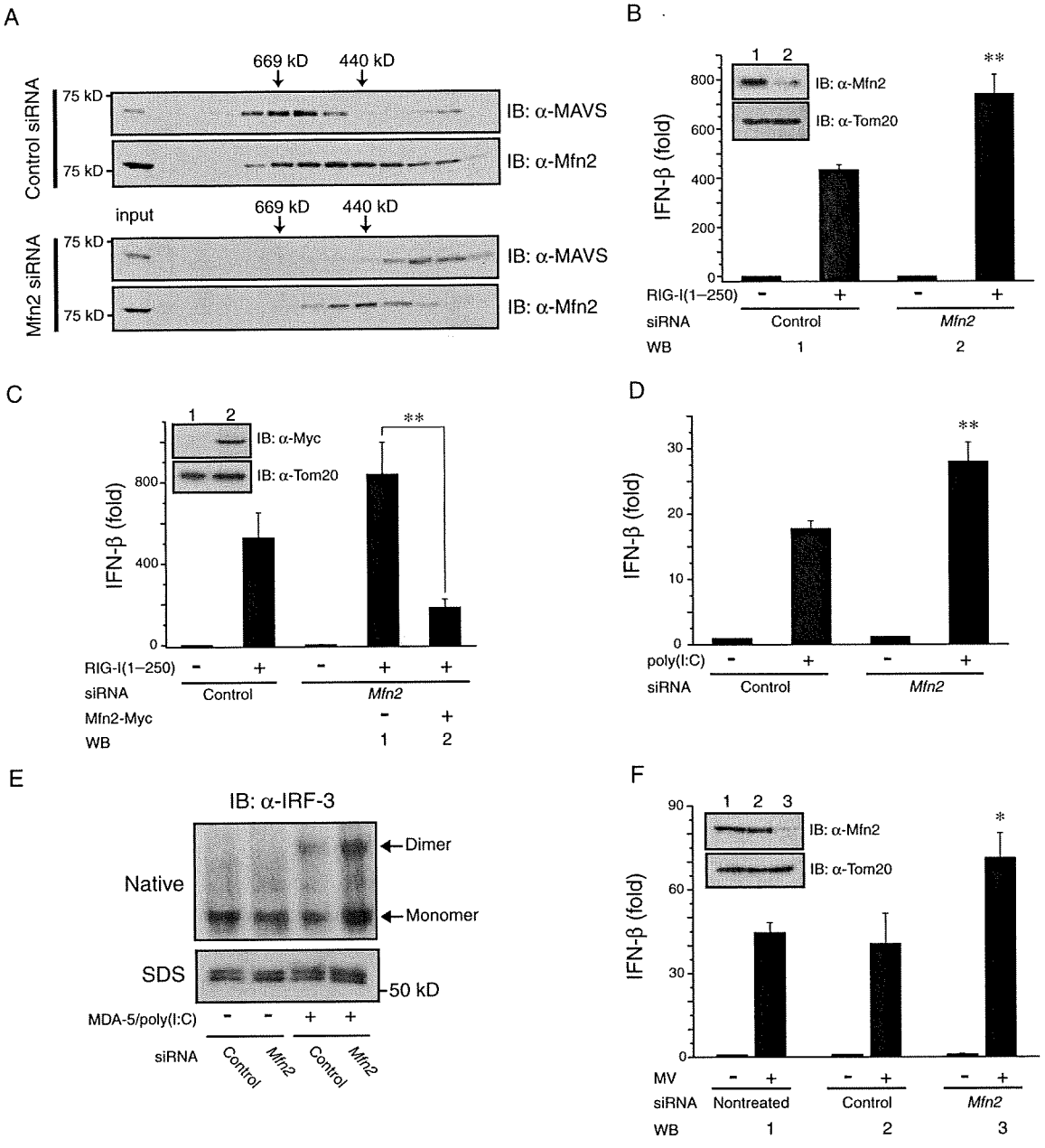

Fig. 4. Treatment with Mfn2-specific siRNA results in an enhanced antiviral response. (A) Gel filtration (Superose 6 HR-10/30) elution profiles of endogenous Mfn2 (as well as MAVS) extracted from the mitochondrial fraction of HEK 293 cells that had been treated with either control siRNA or siRNA specific for Mfn2. The positions corresponding to the elution of 669- and 440-kD molecular mass markers are indicated, and fractions were analyzed by Western blotting with antibodies against Mfn2 and MAVS. (B) HEK 293 cells were transfected with either control siRNA or siRNA specific for Mfn2 to evaluate the effect of knockdown of Mfn2 on the antiviral response. Twenty-four hours later, siRNA-treated cells were retransfected with the IFN-β reporter plasmid together with a plasmid encoding RIG-I(1–250). The efficiency of knockdown of Mfn2 (inset, lane 2) was confirmed by analysis of Western blots (WB) with a monoclonal antibody against Mfn2, and Tom20 was used as a loading control. (C) Experiments were performed similarly to those described in (B), except that IFN-β reporter-dependent luciferase activity was additionally measured after reintroduction of Myc-tagged Mfn2. Expression of the plasmid encoding Myc-tagged Mfn2 was confirmed by Western blotting analysis with an antibody (9E10) against Myc (inset, lane 2). (D) Experiments were performed similarly to those in (B), except that cells were transfected with poly(I:C) instead of the plasmid encoding RIG-I(1–250). (E) Knockdown of Mfn2 enhanced MDA-5–induced activation of IRF-3. (F) Activation of the IFN-β reporter in siRNA-treated HEK 293 cells infected with measles virus (MV) at an MOI of 2. All data shown represent mean values ± SD (n = 3 experiments). *P < 0.05; **P < 0.01.

protein in response to transfection with poly(I:C) (Fig. 4D and fig. S3), as well as increasing the amount of MDA-5–induced dimerized IRF-3 (Fig. 4E). Consistent with these findings, activation of the IFN-β reporter in response to infection with measles virus (MV), an RNA virus of the *Paramyxoviridae* family, was also enhanced in the cells treated with Mfn2-specific siRNA compared to that in control cells (Fig. 4F).

Given that our knockdown experiments failed to completely deplete Mfn2 protein (the effects were relatively modest), we evaluated IFN-β responses in wild-type (WT) and *Mfn2*-deficient MEFs (*28*). MAVS- and RIG-I–dependent production of IFN-β was significantly enhanced (>4-fold) in the *Mfn2*-deficient cells compared to that of WT cells (Fig. 5A). In addition, reintroduction of Myc-tagged murine Mfn2, but not that of its homolog mMfn1, fully restored suppression of IFN-β production in MEFs from $Mfn2^{-/-}$ mice (Fig. 5B), underscoring the importance of endogenous Mfn2 for the modulation of MAVS-mediated antiviral responses. When the $Mfn2^{-/-}$ MEFs were infected with a recombinant vesicular stomatitis virus (VSV) expressing green fluorescent protein (GFP) (VSVΔG*-G) (*29*), the production of IFN-β protein was substantially increased relative to that of infected WT and *Mfn1*-deficient MEFs (Fig. 5C), and the number of cells expressing GFP was significantly reduced only in the *Mfn2*-deficient MEFs, indicating their increased resistance to VSV infection (Fig. 5D). Furthermore, induction of IFN-β production by a positive-stranded RNA virus of the *Picornavirus* family, encephalomyocarditis virus (EMCV), was also greater in the *Mfn2*-deficient MEFs relative to that of WT MEFs (Fig. 5E), consistent with a role for Mfn2 as an inhibitor of the MAVS-mediated antiviral response.

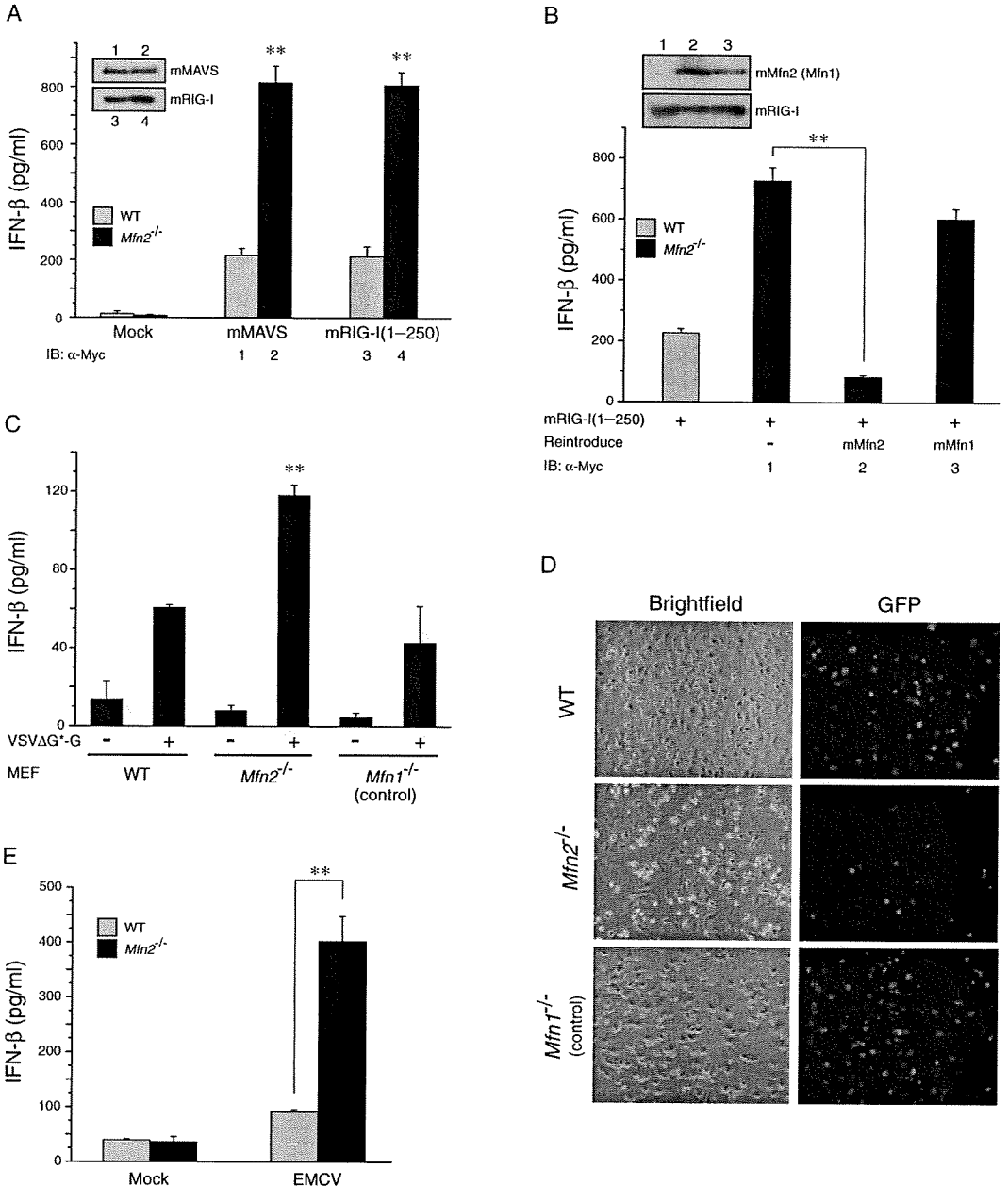

Fig. 5. The effect of Mfn2 deficiency on viral infection in MEFs. (A) WT and *Mfn2*-deficient MEFs were transfected with plasmids encoding either murine MAVS or mRIG-I(1–250), and the production of IFN-β was measured by ELISA 24 hours after transfection. Mock treatment of MEFs involved their transfection with equivalent amounts of pcDNA3.1(–). (B) Reconstitution of *Mfn2*-deficient MEFs with Mfn2 restores modulation of the IFN-β response. *Mfn2*-deficient MEFs were transfected with plasmids encoding mRIG-I(1–250) and either Myc-tagged mMfn2 or mMfn1, and culture supernatants were harvested 24 hours later for measurement of IFN-β production by ELISA. Expression of the plasmids encoding Mfn2 or Mfn1 was confirmed by analysis of Western blots with an antibody against Myc (inset, lanes 2 and 3). (C) This experiment was performed similarly to that described in (A) except that WT and *Mfn2*-deficient MEFs were infected with VSVΔG*-G at an MOI of 3. In this experiment, $Mfn1^{-/-}$ MEFs were also used as a control to evaluate the specificity of Mfn2 in modulating the antiviral response. (D) Fluorescence microscopy (GFP) of MEFs infected with VSVΔG*-G at an MOI of 3 for 24 hours. (E) WT and *Mfn2*-deficient MEFs were infected with EMCV at an MOI of 3, and the production of IFN-β was measured by ELISA. All ELISA data shown represent mean values ± SD ($n = 3$ experiments). $^{**}P < 0.01$.

The HR1 region of Mfn2 is critical for its interaction with MAVS

Through a coimmunoprecipitation approach, we mapped the region of Mfn2 that interacted with MAVS to a central 4,3 hydrophobic heptad repeat (HR1) region (Mfn2-HR1) (Fig. 6A). An analogous approach with deletion mutants of MAVS yielded results indicating that the C-terminal regions of MAVS (amino acid residues 201 to 540) were both necessary and sufficient for the interaction with Mfn2-HR1, and that both the CARD, which is important for the interaction between MAVS and cytoplasmic RNA helicases, and the proline-rich domain were dispensable for this interaction (Fig. 6B). The interaction between Mfn2-HR1 and MAVS was observed only with the transmembrane-anchored form of MAVS (C-term/TM), indicating that the Mfn2-HR1 fragment recognized a structural or topological element (or both) that was specific to the mitochondrial outer membrane–bound form of MAVS.

These results prompted us to investigate the functional role of the HR1 region in the regulation of the antiviral response. In HEK 293 cells, expression of a plasmid encoding the Mfn2-HR1 fragment potently and dose-dependently suppressed IFN-β and NF-κB responses to the overexpression of MAVS-, RIG-I(1–250), and MDA-5 (Fig. 6C and fig. S4) in a manner similar to that observed with full-length Mfn2, indicating that the HR1 region could behave as a dominant-negative modulator of antiviral signaling. Mutations of the predicted *f* position in the HR1 region (E424G and R468H) (fig. S5), which is exposed on the surface of the protein, resulted in a severe loss of function when we evaluated the ability of the mutated protein to modulate the RIG-I–induced IFN-β response, whereas a GTPase mutant of Mfn2 ($Mfn2^{K109A}$) behaved nearly similarly to WT Mfn2 (Fig. 6D). Although the HR1 region has been characterized as an im-

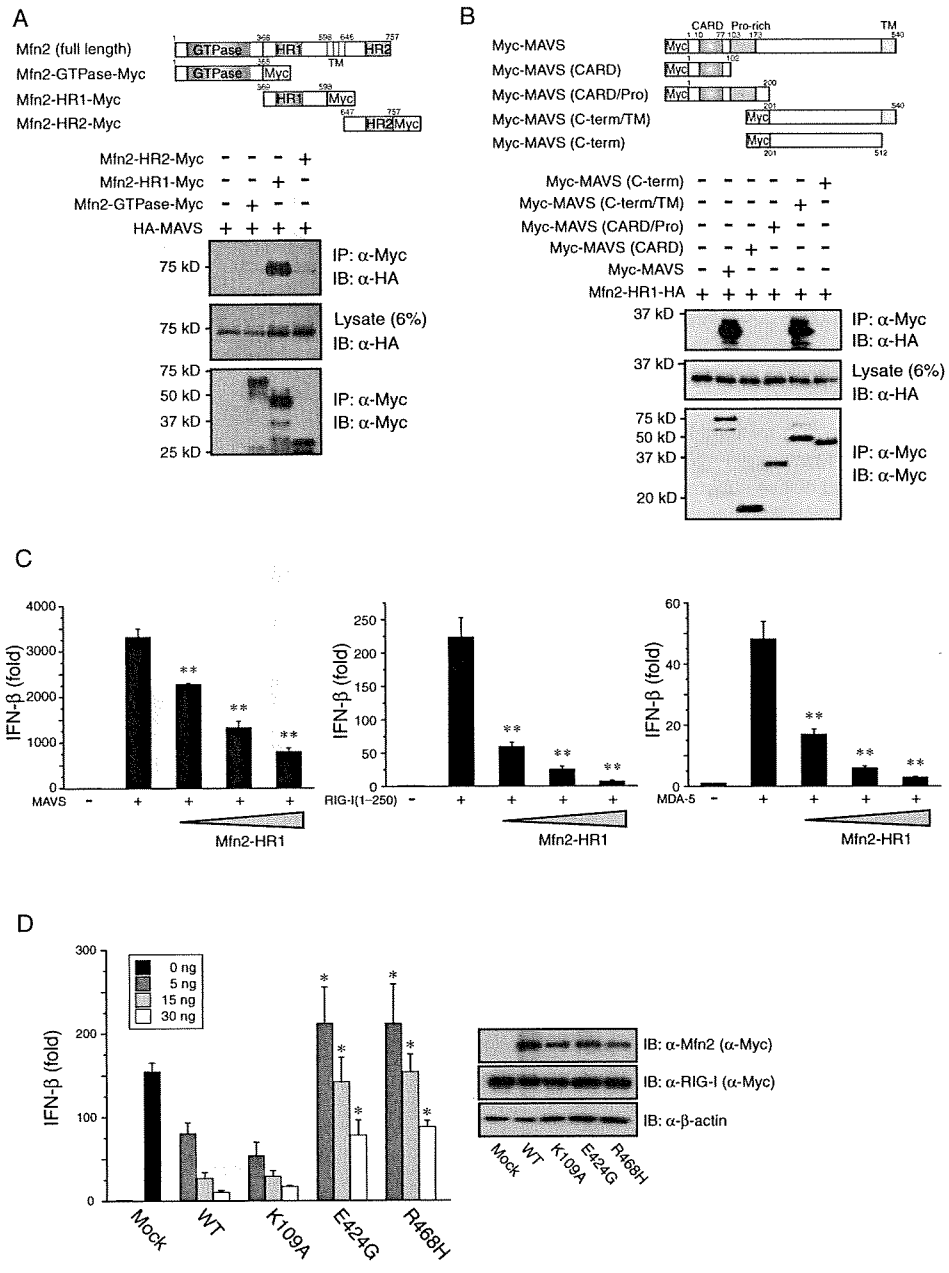

Fig. 6. The HR1 region of Mfn2 associates with MAVS and inhibits activation of the IFN-β reporter. (A) Interaction of HA-tagged MAVS and Myc-tagged Mfn2 variants (upper panel) was analyzed by coimmunoprecipitation assays, which were performed as described for Fig. 1B. The GTPase domain, hydrophobic heptad repeats (HR) 1 and 2, and transmembrane segment (TM) are depicted. (B) Interaction of truncated MAVS variants with the Mfn2-HR1 fragment. (C) HEK 293 cells were cotransfected with 50 ng of plasmids encoding either MAVS, RIG-I(1–250), or MDA-5 together with increasing amounts (20, 50, and 100 ng) of a plasmid encoding the Mfn2-HR1 fragment and the IFN-β luciferase reporter plasmid as described for Fig. 2. (D) HEK 293 cells were cotransfected with 50 ng of plasmid encoding RIG-I(1–250) and increasing amounts (5, 15, and 30 ng; inset) of plasmids encoding WT and mutant Mfn2 proteins together with the IFN-β reporter plasmid. Western blots showing the abundance of the WT and mutant Mfn2 proteins, as well as the abundance of stimulated RIG-I(1–250). All data shown represent mean values ± SD (n = 3 experiments). *P < 0.05; **P < 0.01.

portant domain for mitochondrial targeting (*30*) or fusion (*31*), its functional role in mitofusin homologs is still poorly understood. Our results indicate that the HR1 region of Mfn2 is critical for regulating the antiviral signaling pathway.

Mfn2 functions upstream of TRAF6 and TBK-1

Because Mfn2 was required for regulating antiviral signaling through MAVS, it was likely that Mfn2 acted downstream of (or at the same level as) MAVS in this pathway. In the course of examining the mechanism of its inhibitory activity, we found that Mfn2-specific siRNA had no effect either on the activation of the NF-κB reporter in response to tumor necrosis factor receptor-associated factor 6 (TRAF6) (Fig. 7A), an essential upstream regulator of the inhibitor of κB kinase complex, or on the activation of the IFN-β reporter in response to TANK-binding kinase 1 (TBK-1) (Fig. 7A), a kinase that targets IRF-3, even though both of these effectors act downstream of MAVS (*9*, *15*, *32*, *33*). Consistent with these findings, the production of the proinflammatory cytokine interleukin-6 (IL-6) by TRAF6 was also unaffected in *Mfn2*-deficient MEFs (Fig. 7B), suggesting that Mfn2 inhibited the RIG-I pathway downstream of MAVS and upstream of both TRAF6 (the NF-κB activation pathway) and TBK-1 (the IRF-3 activation pathway).

DISCUSSION

The mitochondrion is well known as the powerhouse of eukaryotic cells, and it is additionally involved in antiviral immunity in vertebrates (*9*–*13*). Despite the central role that the mitochondrial integral membrane protein MAVS plays in this pathway, few additional mitochondrial membrane proteins have been implicated in regulating its activity. In this study, we described our findings that Mfn2, a known mediator of mitochondrial fusion, interacted with MAVS to inhibit antiviral signaling pathways.

Our results show that MAVS forms a stable supramolecular assembly on the outer mitochondrial membrane at physiological pH. We propose that the MAVS complex is an Mfn2-dependent complex because knockdown of endogenous Mfn2 reduced the apparent molecular mass of MAVS, as determined by analytical size exclusion chromatography, from ~600 kD to a lower molecular mass (Fig. 4A). Because loss of endogenous Mfn2 also enhanced the MAVS-mediated antiviral response, it is possible that rearrangement of MAVS from a higher- to a lower-order complex is a prerequisite for the activation of MAVS in response to upstream signaling from RIG-I or MDA-5. Such a model would suggest that Mfn2 functions by stably sequestering MAVS in nonproductive higher-order complexes that are incapable of propagating a downstream antiviral response. A small portion of MAVS did not colocalize with Mfn2, as observed by both size exclusion chromatography (Fig. 4A) and immunofluorescence microscopy (Fig. 1D), raising the possibility that this fraction represents an available pool of MAVS that could be easily activated on viral infection. At present, it is unclear whether the lower-order state is more favorable for recruiting downstream molecules such as TRAF family members or whether it is preferentially competent for signaling to the IRF-3 or NF-κB activation pathways.

In conclusion, we propose a mechanism for the regulation of the cellular antiviral response in which signaling events at the mitochondrial outer membrane involving MAVS are modulated by Mfn2 through its HR1

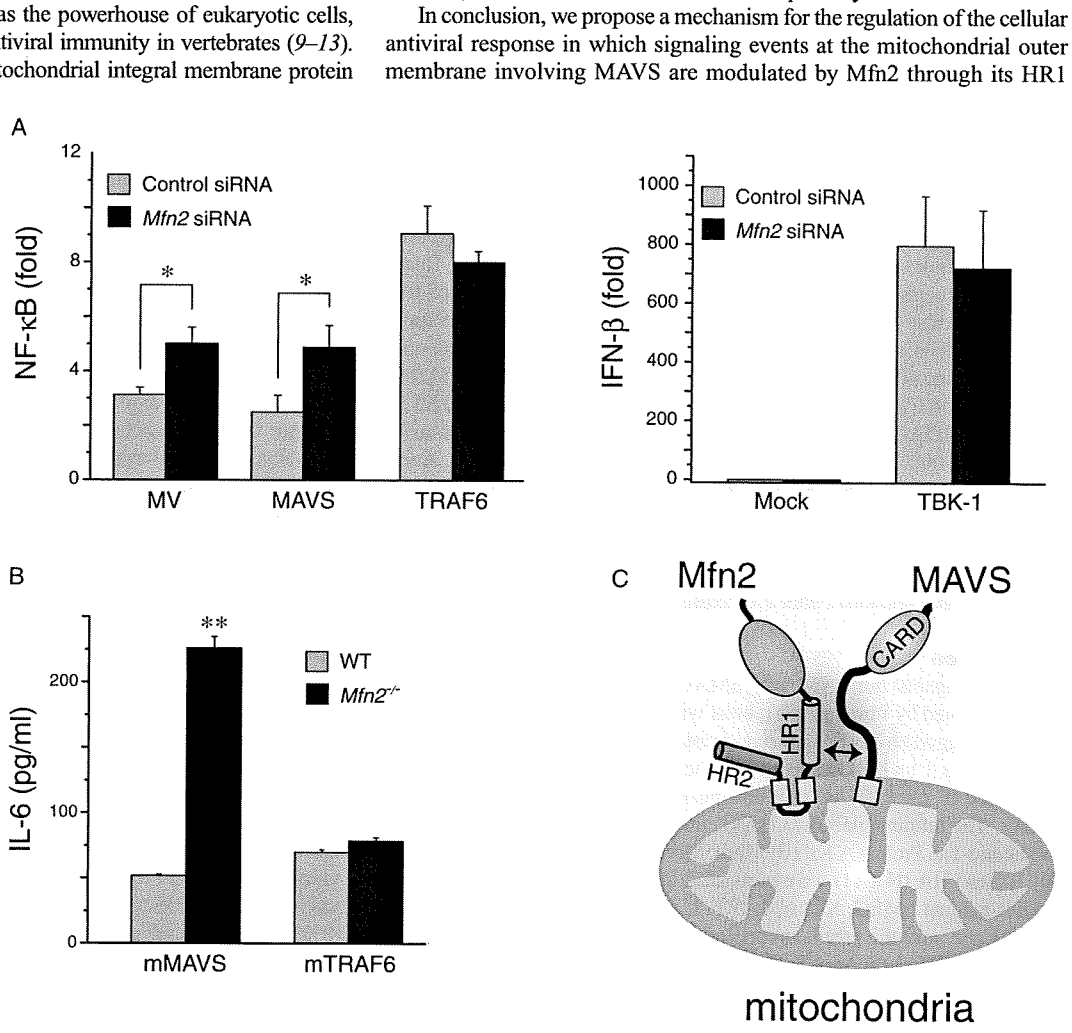

Fig. 7. The role of Mfn2 in antiviral signaling. (A) Activation of NF-κB (left panel) and IFN-β (right panel) reporters in siRNA-treated HEK 293 cells transfected with plasmids encoding MAVS, TRAF6, or TBK-1. In the control (left panel), cells were infected with measles virus (MV) at an MOI of 2. (B) WT and *Mfn2*-deficient MEFs were transfected with plasmids encoding either mMAVS or mTRAF6, and the subsequent production of IL-6 was measured by ELISA. All data shown represent mean values ± SD ($n = 3$ experiments). *$P < 0.05$; **$P < 0.01$. (C) Schematic representation of the MAVS-Mfn2 interaction on the mitochondrial outer membrane.

region (Fig. 7C) upon formation of a supramolecular complex. In this model, we speculate that Mfn2 inhibits the function of the C-terminal region (including the transmembrane domain) of MAVS rather than blocks its CARD, in contrast to previous findings with NOD-like receptor (NLR) family member X1 (NLRX1), a member of the cytoplasmic NLR family that also modulates MAVS-dependent antiviral signaling (*11*). Moreover, it is noteworthy that inhibition of MAVS-mediated antiviral signaling was not observed with Mfn1, which suggests that Mfn1 and Mfn2 are not functionally redundant and illustrates that Mfn2 has multiple specialized functions in the cell (*22–24*, *34*). A small amount of Mfn2 is thought to be present in the ER (*22*). In addition, stimulator of interferon genes (STING) [also termed MITA (*13*)], an essential mediator of the activation of IRF-3, is also present in the ER, mitochondria, or both and interacts with MAVS (*35*). Collectively, these findings raise questions about the interplay between the ER and mitochondria that control antiviral signaling and raise the possibility that Mfn2 may be involved.

MATERIALS AND METHODS

Cell culture

The HEK 293 and HeLa cell lines were maintained in Dulbecco's modified Eagle's medium (DMEM, GIBCO BRL) supplemented with 1% L-glutamine, 1% penicillin-streptomycin, and 10% bovine calf serum or 10% fetal calf serum, respectively, at 5% CO_2 and 37°C. WT, *Mfn1*$^{-/-}$, and *Mfn2*$^{-/-}$ MEFs were provided by D. Chan (Howard Hughes Medical Institute, Caltech) and maintained in standard medium (DMEM supplemented with 10% bovine calf serum) as described previously (*28*). Immunofluorescence microscopy to visualize mitochondria was performed as described previously (*19*, *28*).

Plasmid constructions and mutagenesis

Total messenger RNA (mRNA) from HEK 293 and MEFs was isolated with the TRIzol reagent (Invitrogen) and reverse-transcribed with moloney murine leukemia virus reverse transcriptase (Wako Pure Chemical Industries, Tokyo, Japan). Polymerase chain reaction assays were performed with PrimeSTAR DNA polymerase (Takara, Tokyo, Japan). The following primers (see Supplementary Materials for sequences) were used to generate the complete open reading frames of human MAVS: TK349/TK356; hMfn2: TK365/TK366; hMfn1: TK363/TK364; hFis1: TK367/TK368; hRIG-I(1–250): TK357/TK358; hMDA-5: TK442/TK443; hTBK-1: TK497/TK498; murine MAVS: TK300/TK307; and mRIG-I(1–250): TK310/TK345. Plasmids encoding epitope-tagged MAVS proteins were constructed by ligating the MAVS cDNA into Not I– and Eco RV–digested pcDNA3.1(−) vector (Invitrogen) that encoded either an N-terminal 3× Myc or 3× hemagglutinin (HA) tag. The hMfn2, hMfn1, hRIG-I(1–250), and hMDA-5 cDNAs were ligated into pcDNA3.1 that encoded either a C-terminal 7× Myc or a 3× HA tag.

Antibodies

Antibodies against human MAVS (hMAVS) and murine MAVS (mMAVS) were generated by immunizing rabbits with either recombinant N-terminal histidine-tagged hMAVS (amino acid residues 1 to 175) or mMAVS (amino acid residues 1 to 173), respectively. The recombinant proteins were overexpressed in *Escherichia coli* and purified from solubilized inclusion bodies. The immunoglobulin G (IgG) fractions were affinity-purified with the Econo-Pac Protein A Kit (BioRad). Monoclonal antibodies against Myc (9E10) and HA (HA.11) were purchased from Covance. Monoclonal antibodies against hMfn2, hTom20, IRF-3, and β-actin were obtained from Santa Cruz, and the rabbit monoclonal antibody (4D4G) against phosphorylated IRF-3 (at Ser^{396}) was from Cell Signaling. The Alexa Fluor 568–conjugated monoclonal antibody against mouse IgG was purchased from Molecular Probes. Polyclonal antibody against hFis1 was from ALEXIS Biochemicals. The monoclonal antibody against mitochondrial heat shock protein 70 (mtHsp70) was from Affinity BioReagents. The polyclonal antibody against rat Mfn2 was a gift from K. Mihara (Kyushu University, Japan).

Analytical size exclusion chromatography

Three 10-cm dishes of confluent HEK 293 cells were washed once with cold 1× phosphate-buffered saline (PBS) (pH 7.2), and cells were scraped off and lysed in 1 ml of homogenization buffer [20 mM Hepes (pH 7.5), 70 mM sucrose, and 220 mM mannitol] by 30 strokes in a Dounce homogenizer. The homogenate was centrifuged at 800*g* for 5 min to precipitate nuclei, and the resulting supernatant was further centrifuged at 10,000*g* for 10 min at 4°C to precipitate the crude mitochondrial fraction. After the pellet was washed once with homogenization buffer, the mitochondrial extracts were prepared by solubilization with lysis buffer [50 mM tris-HCl (pH 7.2), 200 mM NaCl, 10% glycerol, and 1% digitonin] and clarification by centrifugation at 12,000*g* for 5 min. Size exclusion chromatography of mitochondrial extracts was performed on Superdex-200 HR-10/30 or Superose 6 HR-10/30 columns (GE Healthcare) equilibrated with 50 mM tris-HCl (pH 7.2) containing 200 mM NaCl, 10% glycerol, and 0.1% NP-40. Extracts were loaded onto the column at a flow rate of 0.3 ml/min at room temperature. Fractions (600 μl each) were collected, resolved by 8% SDS–polyacrylamide gel electrophoresis (SDS-PAGE), and analyzed by Western blotting with either a polyclonal antibody against hMAVS (see above) or a monoclonal antibody against hMfn2. For the analysis of Fis1, fractions were resolved by 15% SDS-PAGE followed by Western blotting analysis with a polyclonal antibody against hFis1. The following molecular weight standards (GE Healthcare) were used: Blue Dextran-2000 (2000 kD), thyroglobulin (669 kD), ferritin (440 kD), catalase (232 kD), and bovine serum albumin (67 kD).

Immunoprecipitation of the hMAVS complex

HEK 293 cells were transfected with the expression plasmid encoding 3× Myc-tagged hMAVS (see above) by the calcium phosphate method. Transfected cells were selected in DMEM medium supplemented with hygromycin B (200 μg/ml; Wako Pure Chemical Industries) for 2 weeks. Stably transfected cells were grown to confluence on five 15-cm dishes. Cells were washed three times with 1× PBS (pH 7.2) and lysed with 10 ml of lysis buffer [20 mM Hepes (pH 7.5), 150 mM NaCl, 10% glycerol, 1 mM EDTA, 1 mM DTT, and 1% digitonin] supplemented with Complete Mini Protease Inhibitor Cocktail (Roche). The clarified supernatant was incubated with monoclonal antibody against the Myc tag (9E10) at 4°C for 2 hours, after which 60 μl of protein A–Sepharose beads (GE Healthcare) was added. After incubation for 5 hours at 4°C, the beads were washed three times with lysis buffer, and immunoprecipitates were resolved by 10% SDS-PAGE. Silver-stained bands were analyzed by LC/MS/MS (Medical Institute of Bioregulation, Kyushu University, Japan).

Coimmunoprecipitations

Coimmunoprecipitation experiments were performed as described previously (*36*) with minor modifications. HEK 293 cells at 80% confluence were transiently transfected with the appropriate plasmids (2 μg each) in a six-well plate by the calcium phosphate method. Two days after transfection, cells were lysed with 1 ml of lysis buffer [50 mM tris-HCl (pH 7.4), 150 mM NaCl, 10% glycerol, and 1% NP-40], and the clarified supernatants were incubated overnight at 4°C with 20 μl of agarose beads (Sigma-Aldrich) conjugated to a polyclonal antibody against *c*-Myc. After four washes with 1× PBS (pH 7.2), immunoprecipitates were resolved by 8 or 12% SDS-PAGE and analyzed by Western blotting with a monoclonal antibody (HA.11) against the HA tag followed by a horseradish peroxidase (HRP)-conjugated antibody against mouse IgG (Jackson ImmunoResearch). To immunoprecipitate endogenous MAVS, HEK 293 cells and MEFs were

lysed with 1% digitonin lysis buffer, and the clarified supernatants were incubated with 10 μg of antibody against hMAVS or mMAVS, followed by incubation overnight at 4°C with 20 μl of protein A–Sepharose beads. The beads were washed four times with lysis buffer, and immunoprecipitates were resolved by 8% SDS-PAGE, analyzed by Western blotting with a monoclonal antibody against hMfn2, and detected with a HRP-conjugated antibody against mouse IgG.

Luciferase assays

HEK 293 cells (2×10^5 cells per well) were plated in 24-well plates. The following day, cells were cotransfected with 100 ng of a luciferase reporter plasmid (p125luc or pELAM), 2.5 ng of the *Renilla* luciferase internal control vector phRL-TK (Promega), and each of the indicated plasmids with the Lipofectamine 2000 reagent (Invitrogen). Empty vector [pcDNA3.1(−)] was used to maintain equivalent amounts of DNA in each well. Cells were harvested 24 hours after transfection and analyzed by a dual-luciferase reporter assay on the GloMax 20/20n luminometer (Promega). Each experiment was replicated at least three times. The p125luc reporter plasmid was provided by T. Taniguchi (University of Tokyo, Japan).

Native PAGE

Native PAGE experiments were performed as described previously (*37*).

RNA interference

For RNA interference–based knockdown experiments, a 25-nucleotide siRNA was purchased from Invitrogen (Stealth Select RNAi). HEK 293 cells were transfected with 50 nM siRNA (final concentration) with Lipofectamine RNAiMAX (Invitrogen). The following day, cells were transfected with luciferase reporter plasmids and then harvested after an additional 24 hours. The designation and sequence (sense strand only) of the Stealth Select RNAi oligonucleotides used in the study were hMfn2 (HSS115028) and 5′-ggaccuccaugggcauucuuguugu-3′, respectively. Stealth RNAi Negative Control Medium GC Duplex #2 (Invitrogen) was used as the control.

ELISA

Production of IFN-β by HEK 293 cells and MEFs was measured with species-specific ELISA reagents for human and murine IFN-β from Kamakura Techno-Science Inc. (Kanagawa, Japan) and PBL Biomedical Laboratories, respectively. The ELISA kit for murine IL-6 was purchased from R&D Systems.

Viral infections

The siRNA-treated HEK 293 cells, which were also cotransfected with reporter plasmids, were plated in 12-well plates and incubated overnight. When the cells were 50% confluent, the culture medium was aspirated and the cells were infected with 200 μl of the Edmonston strain of measles virus (*38*) at 37°C at a multiplicity of infection (MOI) of 2. One hour after infection, cells were supplemented with 800 μl of standard DMEM, then incubated for another 48 hours before the performance of luciferase assays. MEFs were infected with either VSVΔG*-G (*29*) or EMCV (*25*) at an MOI of 3 and incubated for 24 hours before analysis by ELISA, as described above.

SUPPLEMENTARY MATERIALS

www.sciencesignaling.org/cgi/content/full/2/84/ra47/DC1

Materials

Fig. S1. Interaction between endogenous mMfn2 and mMAVS in MEFs.

Fig. S2. Knockdown of Mfn2 with specific siRNA results in enhanced MAVS-mediated activation of the IFN-β reporter.

Fig. S3. Treatment of HEK 293 cells with Mfn2-specific siRNA increased the production of endogenous IFN-β in response to transfection with poly(I:C).

Fig. S4. Mfn2-HR1 is a dominant-negative modulator of MAVS-mediated activation of NF-κB.

Fig. S5. Sequence alignment of Mfn2 homologs within HR1.

Table S1. List of mitochondrial proteins, other than Mfn2, that were identified by LC/MS/MS.

Reference

REFERENCES AND NOTES

1. J. A. Hoffmann, F. C. Kafatos, C. A. Janeway Jr., R. A. B. Ezekowitz, Phylogenetic perspectives in innate immunity. *Science* **284**, 1313–1318 (1999).
2. S. Akira, K. Takeda, T. Kaisho, Toll-like receptors: Critical proteins linking innate and acquired immunity. *Nat. Immunol.* **2**, 675–680 (2001).
3. T. Kawai, S. Akira, Innate immune recognition of viral infection. *Nat. Immunol.* **7**, 131–137 (2006).
4. A. Le Bon, D. F. Tough, Links between innate and adaptive immunity via type I interferon. *Curr. Opin. Immunol.* **14**, 432–436 (2002).
5. A. Iwasaki, R. Medzhitov, Toll-like receptor control of the adaptive immune responses. *Nat. Immunol.* **5**, 987–995 (2004).
6. X. Wang, The expanding role of mitochondria in apoptosis. *Genes Dev.* **15**, 2922–2933 (2001).
7. S. Raha, B. H. Robinson, Mitochondria, oxygen free radicals, disease and ageing. *Trends Biochem. Sci.* **25**, 502–508 (2000).
8. G. A. Rutter, R. Rizzuto, Regulation of mitochondrial metabolism by ER Ca^{2+} release: An intimate connection. *Trends Biochem. Sci.* **25**, 215–221 (2000).
9. R. B. Seth, L. Sun, C. K. Ea, Z. J. Chen, Identification and characterization of MAVS, a mitochondrial antiviral signaling protein that activates NF-κB and IRF3. *Cell* **122**, 669–682 (2005).
10. X. D. Li, L. Sun, R. B. Seth, G. Pineda, Z. J. Chen, Hepatitis C virus protease NS3/4A cleaves mitochondrial antiviral signaling protein off the mitochondria to evade innate immunity. *Proc. Natl. Acad. Sci. U.S.A.* **102**, 17717–17722 (2005).
11. C. B. Moore, D. T. Bergstralh, J. A. Duncan, Y. Lei, T. E. Morrison, A. G. Zimmermann, M. A. Accavitti-Loper, V. J. Madden, L. Sun, Z. Ye, J. D. Lich, M. T. Heise, Z. Chen, J. P. Ting, NLRX1 is a regulator of mitochondrial antiviral immunity. *Nature* **451**, 573–577 (2008).
12. I. Tattoli, L. A. Carneiro, M. Jéhanno, J. G. Magalhaes, Y. Shu, D. J. Philpott, D. Arnoult, S. E. Girardin, NLRX1 is a mitochondrial NOD-like receptor that amplifies NF-κB and JNK pathways by inducing reactive oxygen species production. *EMBO Rep.* **9**, 293–300 (2008).
13. B. Zhong, Y. Yang, S. Li, Y. Y. Wang, Y. Li, F. Diao, C. Lei, X. He, L. Zhang, P. Tien, H. B. Shu, The adaptor protein MITA links virus-sensing receptors to IRF3 transcription factor activation. *Immunity* **29**, 538–550 (2008).
14. T. Kawai, K. Takahashi, S. Sato, C. Coban, H. Kumar, H. Kato, K. J. Ishii, O. Takeuchi, S. Akira, IPS-1, an adaptor triggering RIG-I- and Mda5-mediated type I interferon induction. *Nat. Immunol.* **6**, 981–988 (2005).
15. L. G. Xu, Y. Y. Wang, K. J. Han, L. Y. Li, Z. Zhai, H. B. Shu, VISA is an adapter protein required for virus-triggered IFN-β signaling. *Mol. Cell* **19**, 727–740 (2005).
16. E. Meylan, J. Curran, K. Hofmann, D. Moradpour, M. Binder, R. Bartenschlager, J. Tschopp, Cardif is an adaptor protein in the RIG-I antiviral pathway and is targeted by hepatitis C virus. *Nature* **437**, 1167–1172 (2005).
17. H. Kumar, T. Kawai, H. Kato, S. Sato, K. Takahashi, C. Coban, M. Yamamoto, S. Uematsu, K. J. Ishii, O. Takeuchi, S. Akira, Essential role of IPS-1 in innate immune responses against RNA viruses. *J. Exp. Med.* **203**, 1795–1803 (2006).
18. Q. Sun, L. Sun, H. H. Liu, X. Chen, R. B. Seth, J. Forman, Z. J. Chen, The specific and essential role of MAVS in antiviral innate immune responses. *Immunity* **24**, 633–642 (2006).
19. A. Jofuku, N. Ishihara, K. Mihara, Analysis of functional domains of rat mitochondrial Fis1, the mitochondrial fission-stimulating protein. *Biochem. Biophys. Res. Commun.* **333**, 650–659 (2005).
20. D. C. Chan, Mitochondrial fusion and fission in mammals. *Annu. Rev. Cell Dev. Biol.* **22**, 79–99 (2006).
21. A. Santel, S. Frank, B. Gaume, M. Herrler, R. J. Youle, M. T. Fuller, Mitofusin-1 protein is a generally expressed mediator of mitochondrial fusion in mammalian cells. *J. Cell Sci.* **116**, 2763–2774 (2003).
22. O. M. de Brito, L. Scorrano, Mitofusin 2 tethers endoplasmic reticulum to mitochondria. *Nature* **456**, 605–610 (2008).
23. K. H. Chen, X. Guo, D. Ma, Y. Guo, Q. Li, D. Yang, P. Li, X. Qiu, S. Wen, R. P. Xiao, J. Tang, Dysregulation of HSG triggers vascular proliferative disorders. *Nat. Cell Biol.* **6**, 872–883 (2004).
24. S. Züchner, I. V. Mersiyanova, M. Muglia, N. Bissar-Tadmouri, J. Rochelle, E. L. Dadali, M. Zappia, E. Nelis, A. Patitucci, J. Senderek, Y. Parman, O. Evgrafov, P. D. Jonghe, Y. Takahashi, S. Tsuji, M. A. Pericak-Vance, A. Quattrone, E. Battologlu, A. V. Polyakov, V. Timmerman, J. M. Schröder, J. M. Vance, Mutations in the mitochondrial GTPase mitofusin 2 cause Charcot-Marie-Tooth neuropathy type 2A. *Nat. Genet.* **36**, 449–451 (2004).

25. M. Yoneyama, M. Kikuchi, T. Natsukawa, N. Shinobu, T. Imaizumi, M. Miyagishi, K. Taira, S. Akira, T. Fujita, The RNA helicase RIG-I has an essential function in double- stranded RNA-induced innate antiviral responses. *Nat. Immunol.* **5**, 730–737 (2004).
26. L. Gitlin, W. Barchet, S. Gilfillan, M. Cella, B. Beutler, R. A. Flavell, M. S. Diamond, M. Colonna, Essential role of mda-5 in type I IFN responses to polyriboinosinic: Polyribocytidylic acid and encephalomyocarditis picornavirus. *Proc. Natl. Acad. Sci. U.S.A.* **103**, 8459–8464 (2006).
27. H. Kato, O. Takeuchi, S. Sato, M. Yoneyama, M. Yamamoto, K. Matsui, S. Uematsu, A. Jung, T. Kawai, K. J. Ishii, O. Yamaguchi, K. Otsu, T. Tsujimura, C. S. Koh, C. Reis e Sousa, Y. Matsuura, T. Fujita, S. Akira, Differential roles of MDA5 and RIG-I helicases in the recognition of RNA viruses. *Nature* **441**, 101–105 (2006).
28. H. Chen, S. A. Detmer, A. J. Ewald, E. E. Griffin, S. E. Fraser, D. C. Chan, Mitofusins Mfn1 and Mfn2 coordinately regulate mitochondrial fusion and are essential for embryonic development. *J. Cell Biol.* **160**, 189–200 (2003).
29. A. Takada, C. Robison, H. Goto, A. Sanchez, K. G. Murti, M. A. Whitt, Y. Kawaoka, A system for functional analysis of Ebola virus glycoprotein. *Proc. Natl. Acad. Sci. U.S.A.* **94**, 14764–14769 (1997).
30. M. Rojo, F. Legros, D. Chateau, A. Lombès, Membrane topology and mitochondrial targeting of mitofusins, ubiquitous mammalian homologs of the transmembrane GTPase Fzo. *J. Cell Sci.* **115**, 1663–1674 (2002).
31. E. E. Griffin, D. C. Chan, Domain interactions within Fzo1 oligomers are essential for mitochondrial fusion. *J. Biol. Chem.* **281**, 16599–16606 (2006).
32. S. M. McWhirter, B. R. Tenoever, T. Maniatis, Connecting mitochondria and innate immunity. *Cell* **122**, 645–647 (2005).
33. R. Yoshida, G. Takaesu, H. Yoshida, F. Okamoto, T. Yoshioka, Y. Choi, S. Akira, T. Kawai, A. Yoshimura, T. Kobayashi, TRAF6 and MEKK1 play a pivotal role in the RIG-I-like helicase antiviral pathway. *J. Biol. Chem.* **283**, 36211–36220 (2008).
34. S. Pich, D. Bach, P. Briones, M. Liesa, M. Camps, X. Testar, M. Palacin, A. Zorzano, The Charcot-Marie-Tooth type 2A gene product, Mfn2, up-regulates fuel oxidation through expression of OXPHOS system. *Hum. Mol. Genet.* **14**, 1405–1415 (2005).
35. H. Ishikawa, G. N. Barber, STING is an endoplasmic reticulum adaptor that facilitates innate immune signalling. *Nature* **455**, 674–678 (2008).
36. T. Koshiba, S. A. Detmer, J. T. Kaiser, H. Chen, J. M. McCaffery, D. C. Chan, Structural basis of mitochondrial tethering by mitofusin complexes. *Science* **305**, 858–862 (2004).
37. T. Iwamura, M. Yoneyama, K. Yamaguchi, W. Suhara, W. Mori, K. Shiota, Y. Okabe, H. Namiki, T. Fujita, Induction of IRF-3/-7 kinase and NF-κB in response to double-stranded RNA and virus infection: Common and unique pathways. *Genes Cells* **6**, 375–388 (2001).
38. Y. Yanagi, M. Takeda, S. Ohno, Measles virus: Cellular receptors, tropism and pathogenesis. *J. Gen. Virol.* **87**, 2767–2779 (2006).
39. We are grateful to D. Chan (Howard Hughes Medical Institute and California Institute of Technology, Pasadena, CA) for helpful discussions and for providing wild-type, *Mfn1*-, and *Mfn2*-deficient MEF cell lines. We are also grateful to J. Kulman (Puget Sound Blood Center, Seattle, WA) and K. Mihara (Kyushu University, Japan) for their valuable comments on the study. We thank M. Matsumoto and M. Oda (Kyushu University) for the LC/MS/MS analysis, and Y. Fuchigami for technical assistance with DNA sequencing. The p125luc reporter plasmid was provided by T. Taniguchi (University of Tokyo, Japan). We also thank A. Yoshimura and T. Kobayashi (Keio University, Japan) for providing the FLAG-mTRAF6 expression plasmid, and T. Fujita and M. Yoneyama (Kyoto University, Japan) for EMCV. K.Y. was supported by an Academic Challenge grant by Venture Business Laboratory, Kyushu University. This work was supported by the grants-in-aid for Young Scientists (B) from the Ministry of Education, Culture, Sports, Science, and Technology of Japan (20770123), Kyushu University Interdisciplinary Programs in Education and Projects in Research Development (P & P type D; 20301), and The Uehara Memorial Foundation to T.K. The authors declare that they have no conflict of interest.

Submitted 24 February 2009
Accepted 31 July 2009
Final Publication 18 August 2009
10.1126/scisignal.2000287
Citation: K. Yasukawa, H. Oshiumi, M. Takeda, N. Ishihara, Y. Yanagi, T.Seya, S. Kawabata, T. Koshiba, Mitofusin 2 inhibits mitochondrial antiviral signaling. *Sci. Signal.* **2**, ra47 (2009).

Published August 31, 2009

JEM

BRIEF DEFINITIVE REPORT

Epstein-Barr virus (EBV)–encoded small RNA is released from EBV-infected cells and activates signaling from toll-like receptor 3

Dai Iwakiri,[1] Li Zhou,[1] Mrinal Samanta,[1] Misako Matsumoto,[2] Takashi Ebihara,[2] Tsukasa Seya,[2] Shosuke Imai,[3] Mikiya Fujieda,[4] Keisei Kawa,[5] and Kenzo Takada[1]

[1]Department of Tumor Virology, Institute for Genetic Medicine, Hokkaido University, Sapporo 060-0815, Japan
[2]Department of Microbiology and Immunology, Hokkaido University Graduate School of Medicine, Sapporo 060-8638, Japan
[3]Department of Microbiology and [4]Department of Pediatrics, Kochi Medical School, Kochi University, Nangoku 783-8505, Japan
[5]Osaka Medical Center and Research Institute for Maternal and Child Health, Izumi 594-1101, Japan

Epstein-Barr virus–encoded small RNA (EBER) is nonpolyadenylated, noncoding RNA that forms stem-loop structure by intermolecular base-pairing, giving rise to double-stranded RNA (dsRNA)–like molecules, and exists abundantly in EBV-infected cells. Here, we report that EBER induces signaling from the Toll-like receptor 3 (TLR3), which is a sensor of viral double-stranded RNA (dsRNA) and induces type I IFN and proinflammatory cytokines. A substantial amount of EBER, which was sufficient to induce signaling from TLR3, was released from EBV-infected cells, and the majority of the released EBER existed as a complex with a cellular EBER-binding protein La, suggesting that EBER was released from the cells by active secretion of La. Sera from patients with infectious mononucleosis (IM), chronic active EBV infection (CAEBV), and EBV-associated hemophagocytic lymphohistiocytosis (EBV-HLH), whose general symptoms are caused by proinflammatory cytokines contained EBER, and addition of RNA purified from the sera into culture medium induced signaling from TLR3 in EBV-transformed lymphocytes and peripheral mononuclear cells. Furthermore, DCs treated with EBER showed mature phenotype and antigen presentation capacity. These findings suggest that EBER, which is released from EBV-infected cells, is responsible for immune activation by EBV, inducing type I IFN and proinflammatory cytokines. EBER-induced activation of innate immunity would account for immunopathologic diseases caused by active EBV infection.

CORRESPONDENCE
Kenzo Takada:
kentaka@igm.hokudai.ac.jp

Abbreviations used: CAEBV, chronic active EBV infection; dsRNA, double-stranded RNA; EBER, EBV-encoded small RNA; EBV-HLH, EBV-associated hemophagocytic lymphohistiocytosis; IM, infectious mononucleosis; IRF, IFN-regulatory factor; La, lupus erythematosis-associated antigen; LCL, lymphoblastoid cell line; PKR, RNA-activated protein kinase; RIG-I, retinoic acid–inducible gene-I; TLR, Toll-like receptor.

Epstein-Barr virus (EBV) is a ubiquitous human herpesvirus that infects >90% of the population. Primary EBV infection is generally asymptomatic; however, when the infection is delayed until adolescence or later, ~50% of cases manifest as infectious mononucleosis (IM). IM is characterized by the expansion of reactive T cells and is most likely to be an immunopathologic disease whose general symptoms are caused by proinflammatory cytokines, such as IL-1, IFN-γ, and TNF (Rickinson and Kieff, 2001). Chronic active EBV infection (CAEBV) and EBV-associated hemophagocytic lymphohistiocytosis (EBV-HLH) are also active EBV infections with persistent or recurrent IM-like symptoms. EBV-HLH is characterized by an EBV infection in T cells and the systemic release of proinflammatory cytokines, which subsequently causes hemophagocytosis of blood cells through the activation of macrophages (Kikuta et al., 1993; Rickinson and Kieff, 2001).

The EBV noncoding RNAs, EBV-encoded RNA 1 (EBER1) and EBER2, are 167 and 172 nt long, respectively, and are expected to form dsRNA-like structures (Rosa et al., 1981). EBER is the most abundant viral transcript in latently EBV-infected cells (Rymo, 1979), and binds to several cellular proteins including

S. Imai's present address is Sapporo Toho Hospital, Sapporo 065-0017, Japan.

The Rockefeller University Press $30.00
J. Exp. Med.
www.jem.org/cgi/doi/10.1084/jem.20081761

Published August 31, 2009

RNA-activated protein kinase (PKR; Clarke et al., 1991), ribosomal protein 22 (L22; Toczyski et al., 1994), lupus erythematosis–associated antigen (La; Lerner et al., 1981), and retinoic acid–inducible gene I (RIG-I; Samanta et al., 2006).

Here, we report that EBER exists in the sera of patients with active EBV infections and induces type I IFN and inflammatory cytokines through TLR3-mediated signaling. This may account for the pathogenesis of active EBV infections that are characterized by cytokinemia.

RESULTS AND DISCUSSION

EBER is present in the culture supernatants of EBV-infected cells

RT-PCR assays have revealed that EBER is present in the culture supernatants of the Burkitt's lymphoma–derived EBV-positive cell lines Mutu+ (Gregory et al., 1990) and Akata+ (Takada, 1984), and the EBV-transformed lymphoblastoid cell lines (LCLs). EBER was detected on day 1 of the culture, and its expression peaked on day 4 (Fig. 1 A). In a real-time PCR assay, 15–35 ng/ml EBER1 was released into the culture supernatants, whereas EBER2 was only faintly detected (Fig. 1 B).

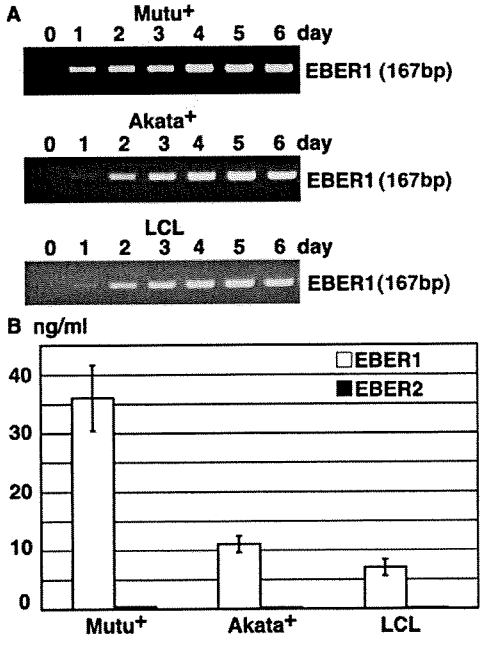

Figure 1. EBER1 is released into the culture supernatants of EBV-infected Mutu+, Akata+ and LCL. (A) RT-PCR of EBER1. Cells (2×10^5 cells/ml) were cultured for the designated number of days. Total RNA was extracted from 1 ml culture supernatant and subjected to 25 cycles of RT-PCR to detect EBER1. Three or more independent experiments were performed. (B) Quantitative RT-PCR of EBER1 and EBER2. Cells (2×10^5) were cultured in 1 ml medium for 4 d, and total RNA was extracted from the culture supernatant and subjected to RT-RCR for the detection of EBER1 and EBER2. Error bars indicate the SD of duplicate wells. The data presented are representative of three independent experiments.

EBER1 induces signaling from TLR3

To investigate the role of the EBER1 that was released from EBV-infected cells, we first examined whether in vitro–synthesized EBER1 could induce signaling from TLR3. RT-PCR assays indicated that LCLs and gastric carcinoma–derived NU-GC-3 cells (Akiyama et al., 1988) expressed TLR3 (Fig. 2 A).The addition of in vitro–synthesized EBER1 into culture medium induced IFN-β in LCLs and EBV-positive and -negative NU-GC-3 cells (Fig. 2 B; Imai et al., 1998). A similar result was also obtained by the TLR3 agonist poly(I:C). An ELISA indicated that IFN-β production was dependent on the amount of EBER1 that was added to the culture supernatants; we found that 0.1 ng/ml EBER1 was sufficient to induce the release of IFN-β (Fig. 2 C). Next, we evaluated the efficiency of EBER1 to induce IFN-β expression in LCLs comparing with poly(I:C). No difference in efficiency was observed between EBER1 and poly(I:C) by RT-PCR (Fig. 2 D).

When LCLs were pretreated with an anti-TLR3 antibody (Matsumoto et al., 2002), and then treated with EBER1, the effect of EBER1 on the induction of IFN-β was markedly reduced (Fig. 2 E). In addition, TLR3 knockdown by siRNA resulted in reduced induction of IFN (Fig. 2 F), indicating that EBER1 induces IFN through TLR3. IFN-regulatory factor 3 (IRF3) and NF-κB function downstream of the TLR3 signaling pathway (Akira and Takeda, 2004). As shown in Fig. 2 G, both IRF3 and NF-κB were phosphorylated upon treatment of the cells with EBER1 or poly(I:C).

We next examined whether the EBER1 that was released into culture supernatants could induce the expression of IFN. Cell culture supernatant was harvested on day 4 and added to the culture medium of LCLs. After 14 h of cultivation, the induction of IFN-β in LCLs was determined by RT-PCR. The results indicated that IFN was induced in EBV-positive cells, but not in EBV-negative cells or EBER-knockout EBV-infected cells (Fig. 2 H).

EBER1 is detected as a complex with La in the culture supernatants, and the complex can induce TLR3 signaling

The stable presence of EBER1 in culture supernatants suggested that EBER1 was bound by some proteins, thus being protected from degradation by nucleases. We then examined whether the EBER1 that was present in culture supernatants existed as a complex with EBER-binding cellular proteins. Flag-tagged L22, La, and PKR were transfected into Mutu+ cells, and their interaction with EBER1 in culture supernatants was examined by coimmunoprecipitation assays. Although flag-tagged L22, La, and PKR were expressed equally in transfected cells, only La could be strongly immunoprecipitated from the culture supernatant (Fig. 3 A). RT-PCR indicated that EBER1 preferentially coimmunoprecipitated with La (Fig. 3 B). The presence of La in culture supernatants suggested that La was actively secreted from living cells rather than passively released from dead cells. These results indicate that EBER1 was released from EBV-infected cells as a complex with La. To further assess whether EBER can activate TLR3 in complexes with La, we used immunoprecipitates

Published August 31, 2009

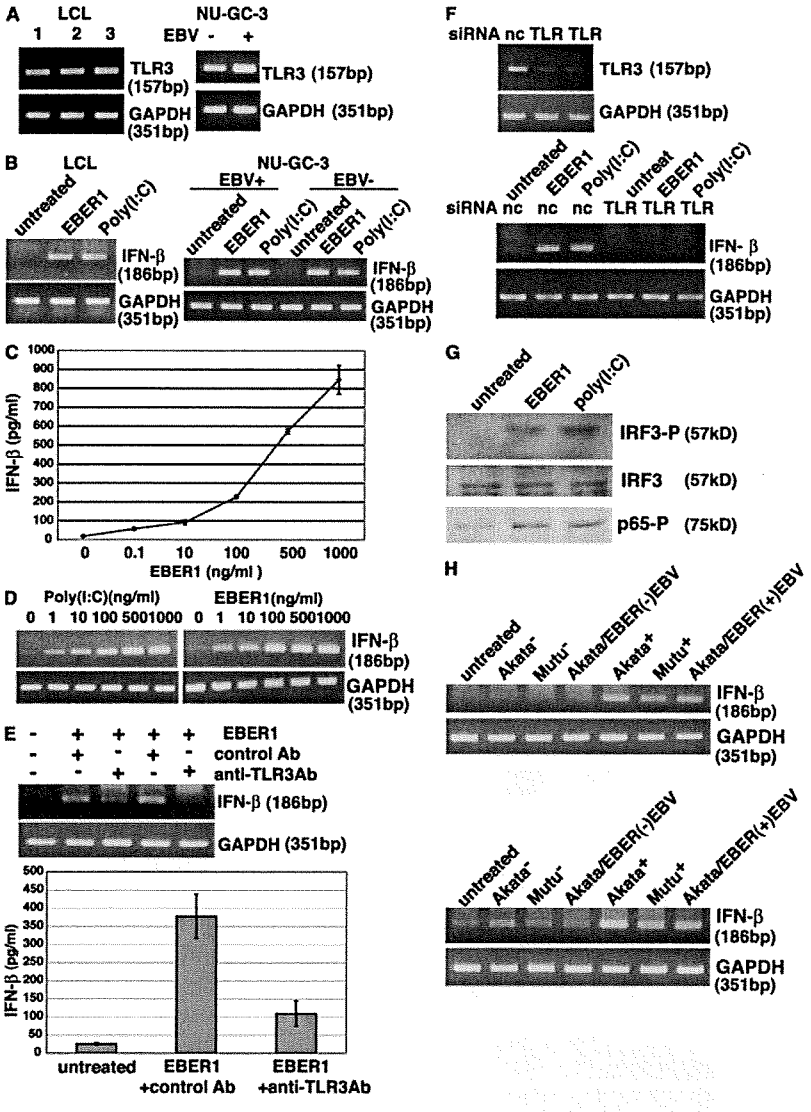

Figure 2. EBER1 activates signaling through TLR3. (A) Detection of TLR3 in three LCL clones and EBV-infected and uninfected NU-GC-3 cells. Total RNA (0.1 μg) was subjected to 30 cycles of RT-PCR to detect TLR3. RT-PCR for GAPDH was used as an internal control. Three or more independent experiments were performed for each assay. (B) Effect of in vitro-synthesized EBER1 on the expression of IFN-β. LCLs and EBV-positive and -negative NU-GC-3 cells were treated with 0.5 μg/ml in vitro-synthesized EBER1 or poly(I:C) and were cultured for 14 h. Total RNA (0.1 μg) was subjected to 30 cycles of RT-PCR to detect IFN-β. RT-PCR for GAPDH was used as an internal control. Three or more independent experiments were performed. (C) Dose response of the effect of in vitro-synthesized EBER1 on the expression of IFN-β. LCLs (4×10^5 cells/ml) were treated with 0.1–1,000 ng/ml EBER1 and cultured for 14 h. IFN-β in culture supernatants was quantified by ELISA. Error bars indicate the S.D. of duplicate wells. The data presented are representative of three independent experiments. (D) Efficiency of EBER1 and poly(I:C) to induce IFN-β expression in LCLs. LCLs (4×10^5 cells/ml) were treated with 1–1,000 ng/ml EBER1 and cultured for 14 h. IFN-β induction was analyzed by RT-PCR. Three or more independent experiments were performed for each assay. (E) Effect of an anti-TLR3 antibody on EBER1-induced IFN-β production. LCLs were preincubated with the anti-TLR3 antibody for 30 min at 37°C, before being treated with 0.5 μg/ml of EBER1 and incubated for 14 h. The culture was analyzed for IFN-β induction by RT-PCR (upper panel) and ELISA (lower panel). Error bars indicate the SD of duplicate wells. The data presented are representative of three independent experiments. (F) Effect of TLR3 knockdown on EBER1-induced IFN-β production. Negative control siRNA (nc) or TLR3-siRNA (TLR) were transfected into EBER-knockout EBV-infected AGS cells. After 48 h, cells were treated with EBER1 or poly(I:C) and IFN-β induction was analyzed by RT-PCR (bottom). Efficiency of TLR3 silencing was analyzed by RT-PCR (top). Three or more independent experiments were performed for each assay. (E) Effect of EBER1 on the downstream signals of TLR3, IRF3, and NF-κB. LCLs were treated with 2.5 μg/ml in vitro-synthesized EBER1 or poly(I:C) and cultured for 3 h before the phosphorylation of IRF3, and NF-κB was examined by immunoblotting using antibodies against phosphorylated IRF3, total IRF3, and phosphorylated p65. The data presented are representative of three independent experiments. (F) Effect of culture supernatants from EBER-positive cells on the expression of IFN-β. The study includes EBV-positive and -negative Mutu cells, EBV-positive and -negative Akata cells, and EBV-negative Akata cells that were stably infected with EBER-positive EBV or EBER-knockout EBV. The cells (2×10^5 cells/ml) were cultured for 4 d and then the culture supernatants were harvested. LCLs (4×10^5) were treated with 1 ml culture supernatants (top) or RNA extracted from 1 ml culture supernatants in 1 ml culture medium (bottom) for 14 h. RNA (0.1 μg) was subjected to 30 cycles of RT-PCR to detect IFN-β. Three or more independent experiments were performed for each assay.

Published August 31, 2009

from culture supernatants of EBV-positive or EBER-knockout EBV-infected cells for stimulation. EBV-positive and EBER-knockout EBV-infected AGS cells were transfected with Flag-La, and immunoprecipitates from culture supernatants were added into a culture medium of EBER-knockout EBV-infected AGS cells. As shown in Fig. 3 C, IFN-β was clearly induced by treatment with immunoprecipitates from culture supernatants of EBV-positive cells, whereas the IFN induction was reduced by TLR3 knockdown. In contrast, no IFN induction was observed in the cells treated with immunoprecipitates from culture supernatants of EBER-knockout EBV-infected cells. These results suggest that EBER1 can induce TLR3 signaling in complexes with La.

EBER1 exists in sera from patients with active EBV infections and induces the production of type I IFN and inflammatory cytokines

Subsequently, we examined the presence of EBER1 in the sera of patients with acute EBV infections, such as IM, CAEBV, and EBV-HLH. We also investigated the role of EBER on the activation of TLR3. Results from RT-PCR assays revealed that EBER1 was detected in patient sera and also in the sera from healthy individuals (Fig. 4 A); however, the level of EBER1 was much higher in patient sera than that obtained from healthy individuals. Our real-time PCR assays indicated that the sera contained 0.17 to 0.24 ng/ml of EBER1 (Fig. 4 B), which was sufficient to induce signaling from TLR3 (Fig. 2 C). Because we had demonstrated that sera nonspecifically induced IFN and cytokines in LCLs, we stimulated LCLs with RNA that had been purified from that sera. As shown in Fig. 4 C, RNAs from the patient sera, which contained a higher amount of EBER1, induced the release of IFN-β when added to the culture medium of LCLs. The quantification of IFN-β by ELISA indicated that all of the patient sera that we examined induced more IFN-β (200–800 pg/ml) than that induced by the sera from healthy individuals. To confirm that IFN-β induction by patient sera was mediated thorough TLR3, LCLs were pretreated with an anti-TLR3 antibody and treated with RNA from a patient serum with IM. The results demonstrate that there was a marked reduction in the RNA-induced release of IFN-β (Fig. 4 D), indicating that the RNA from serum induced the expression of IFN through TLR3. We also examined whether RNAs from the patient sera could induce type I IFN and proinflammatory cytokines such as IFN-γ and TNF in PBMCs. As shown in Fig. 4 E, RNAs purified from CAEBV, which contained a high level of EBER1, induced the expression of IFN-β, IFN-γ, and TNF.

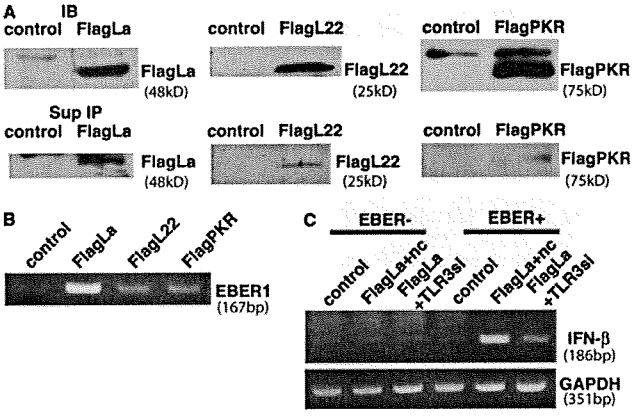

Figure 3. EBER is detected as a complex with La in the culture supernatants and the complex is stimulatory for TLR3. (A) Detection of La, L22, and PKR in culture supernatants. Mutu+ cells (1×10^6) were transfected with Flag-tagged La, L22, or PKR plasmid and cultured for 48 h. Flag-tagged La, L22, and PKR were detected by immunoblotting of the cell lysates (top) and immunoprecipitation of culture supernatants (bottom) using an anti-Flag antibody. Three or more independent experiments were performed for each assay. (B) Detection of EBER1 in the immunoprecipitates. RNA was extracted from the immunoprecipitates and subjected to 30 cycles of RT-PCR to detect EBER1. Three independent experiments were performed. (C) Effect of immunoprecipitates from culture supernatants on IFN-β induction. EBER-positive (EBER+) or EBER-knockout (EBER−) EBV-infected AGS cells were transfected with control (control) or Flag-tagged La plasmid (Flag La) and cultured for 48 h, followed by immunoprecipitation of culture supernatants using anti-Flag antibody. Both EBER− and EBER+ immunoprecipitates were added into the media of EBER-knockout EBV-infected AGS cells transfected with negative control siRNA (Flag La+nc) or TLR3 siRNA (Flag La+TLR3si), and IFN-β induction was analyzed by RT-PCR. The data presented are representative of three independent experiments.

EBER1 induces mature surface phenotype and antigen-presenting capacity of DCs

Finally, we investigated the effect of EBER1 on DC function to clarify whether EBER1-mediated signaling is sufficient for induction of immune responses. We treated immature DCs with EBER1 or poly(I:C) for 24 h and analyzed the surface markers of matured DC by flow cytometry. Treatment with EBER1, as well as poly(I:C), resulted in an increase of CD83 and CD86 levels, indicating that EBER1 induces maturation of DCs (Fig. 5 A). Because CD86 up-regulation by EBER1 was clearly reduced by TLR3 siRNA, EBER1-mediated DC maturation is dependent on TLR3 (Fig. 5 B). We next investigated cytokine production by DCs in response to EBER1. As shown in Fig. 5 C, IFN-β and IL-12 production by DCs was induced by EBER1, indicating EBER1-mediated activation of DCs. Furthermore, sera from patients containing a high level of EBER1 induced IL-12 production by DCs in a TLR3-dependent manner, whereas sera containing a low level of EBER1 or EBV-negative sera could not, suggesting that EBER1 in sera is stimulatory for DCs through TLR3 signaling (Fig. 5 D). To assess whether DCs with maturation induced via EBER1 have the capacity of antigen presentation, DCs treated with EBER1 or poly(I:C) were used for allo MLR assay. The stimulatory properties of EBER1- or poly (I:C)-treated DCs were compared with those of untreated immature DCs. As shown in Fig. 5 E, EBER1- or poly(I:C)-treated DCs induced comparable allo mixed lymphocyte reactions that were most markedly seen with 10,000 DCs/wells, in a 1:10 stimulator/responder ratios. Therefore,

Published August 31, 2009

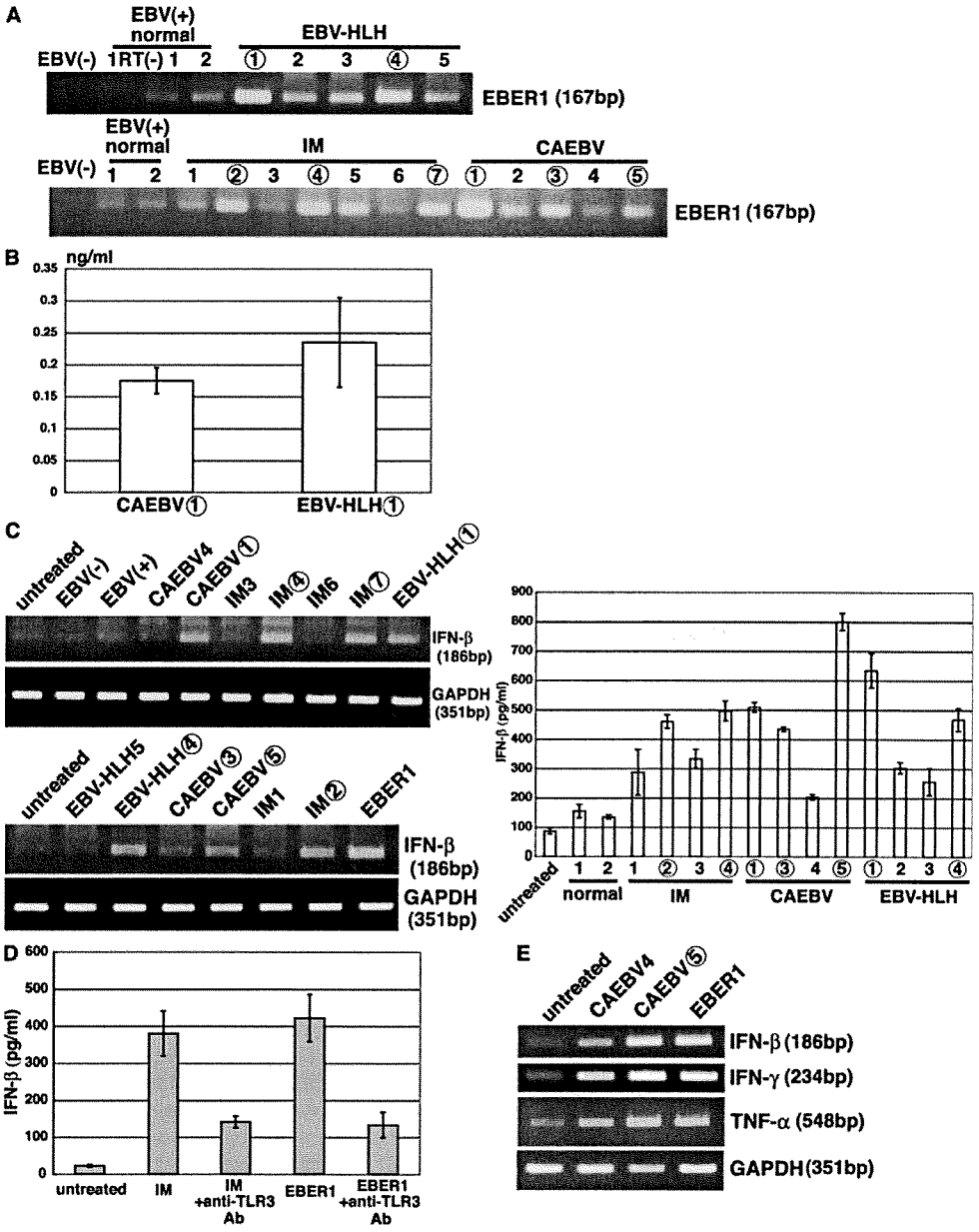

Figure 4. EBER1 exists in sera from patients with active EBV infections and induces the production of type I IFN and inflammatory cytokines. (A) Detection of EBER1 by RT-PCR in patient sera. RNA was extracted from 100 µl sera or plasma from patients with IM, CAEBV, and EBV-HLH, and from EBV-positive and -negative healthy donors. EBER1 was detected by 35 cycles of RT-PCR. Sample numbers in A–C correspond to each other; samples that are followed by a number in an open circle contain higher amounts of EBER1 than those with a number alone. Three or more independent experiments were performed. (B) Quantification of EBER1 in patient sera. RNA was extracted from the sera and subjected to real-time RT-PCR to detect EBER1. Error bars indicate the SD of duplicate wells. The data presented are representative of three independent experiments. (C) Induction of IFN-β production by RNA extracted from patient sera. LCLs (4×10^5) were treated with RNA that had been extracted from 100 µl sera in 1 ml culture medium, incubated for 14 h, and subjected to 30 cycles of RT-PCR to detect IFN-β (left) or ELISA of the culture supernatants for detection of IFN-β (right). The data of ELISA are shown as the means ± SD of duplicate determination and representative results of three independent experiments are shown. (D) Effect of an anti-TLR3 antibody on serum-induced IFN-β production. LCLs (4×10^5) were preincubated with the anti-TLR3 antibody for 30 min at 37°C, before being treated with RNA extracted from 100 µl of serum from a patient with IM or 1.0 µg in vitro–synthesized EBER1 as a positive control in 1 ml culture medium, and cultured for 14 h. Production of IFN-β was determined by ELISA of the culture supernatants. Error bars indicate the S.D. of duplicate wells. The data presented are representative of three independent experiments. (E) Effect of the RNA from patients sera on the induction of IFN-β and proinflammatory cytokines. Human PBMCs (1×10^6) were treated with RNA extracted from 100 µl patients sera or 0.5 µg in vitro–synthesized EBER1 in 1 ml culture medium and cultured for 14 h. The induction of IFN-β and proinflammatory cytokines was determined by 30 cycles of RT-PCR. Three independent experiments were performed.

Published August 31, 2009

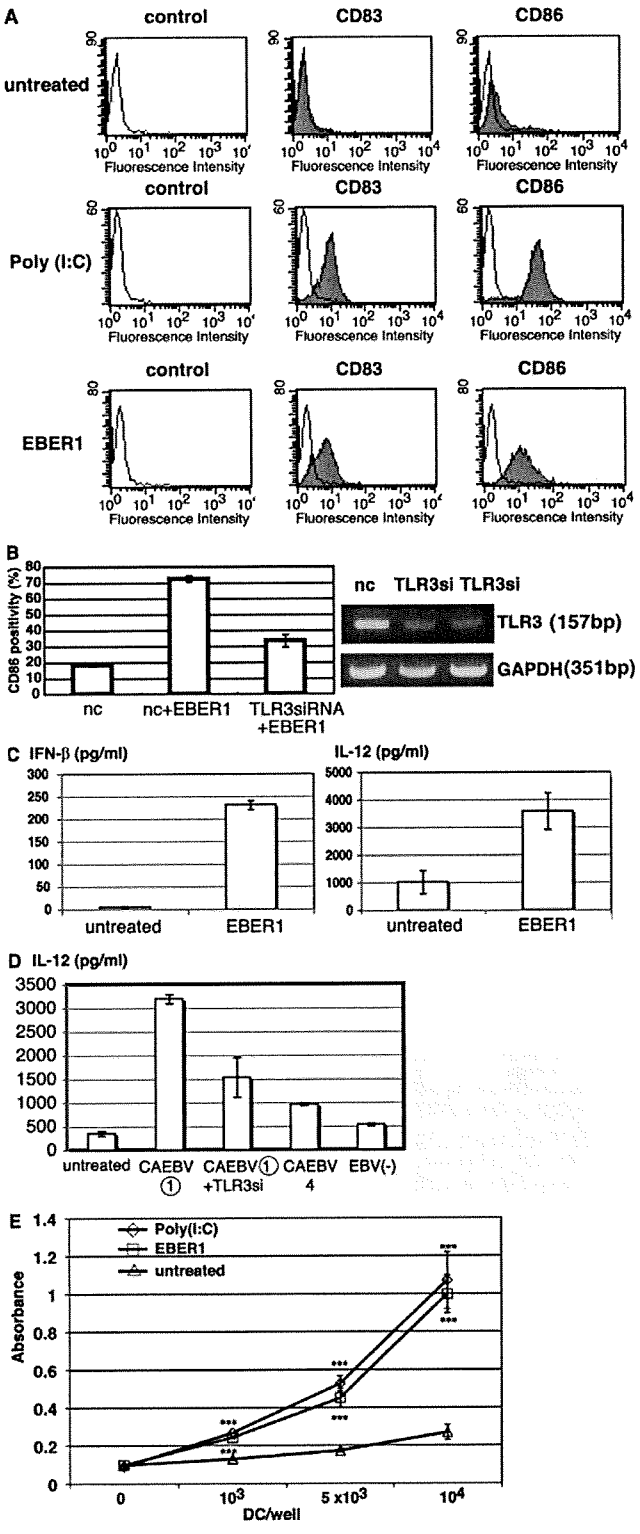

Figure 5. EBER1 induces maturation of DC and subsequent antigen presentation. (A) Effect of EBER1 on phenotype of DCs. DCs were prepared from PBMCs and untreated or treated with either poly(I:C) (10 μg/ml) or EBER1 (10 μg/ml). Surface markers of matured DCs, CD83, and CD86 were measured by flow cytometry. As negative control, cells were stained with mouse IgG. The data are representative of three independent experiments. (B) Effect of TLR3 knockdown on EBER1-mediated DC maturation. DCs were transfected with TLR3 siRNA or control siRNA (nc) and were stimulated with EBER1. CD86 positivity (%) was analyzed by flow cytometry (left). Efficiency of TLR3 silencing was analyzed by RT-PCR (right). Data are shown as the means ± SD of duplicate determination and representative results of three independent experiments are shown. (C) EBER1-induced cytokine production by DCs. DCs were treated with EBER1, and IFN-β or IL-12p40 production were measured by ELISA. Error bars indicate the SD of duplicate wells, and the data presented are representative of three independent experiments. (D) Effect of sera from patients on TLR3-mediated IL-12 production by DCs. DCs were transfected with negative control siRNA or TLR3 siRNA (TLR3si) for 48 h, and then stimulated with sera from patients with CAEBV containing high amounts of EBER1 (CAEBV (1)) and IL-12 production was measured by ELISA. Sera form patients with CAEBV containing low amounts of EBER1 (CAEBV4) or EBV-negative (EBV(−)) healthy donor were also used for stimulation. Data are shown as the means ± SD of duplicate determination and representative results of three independent experiments are shown. (E) Allogenic MLR. DCs treated with either poly(I:C) or EBER1 were used as stimulator cells. Untreated immature DC were also used as stimulator cells. Allogenic PBMCs (1×10^5) were used as responder cells in triplicate cultures. Proliferation of alloreactive T cells was determined by cell proliferation assay. Data are shown as the means ± SD of triplicate determination and representative results of three independent experiments are shown. Statistical significance differences between groups were evaluated by Student's *t* test. ***, $P < 0.001$.

EBER1-treated DCs were potent inducers of primary allo T cell responses.

In this study, we have demonstrated that EBER1 is released from EBV-infected cells and activates signaling from the TLR3. We have also demonstrated that sera from patients with active EBV infections such as IM, CAEBV, and EBV-HLH contained a large amount of EBER1, which was sufficient to activate TLR3 signaling, subsequently resulting in the induction of type I IFN and proinflammatory cytokines. Furthermore, EBER1-treated DCs could induce primary immune response, suggesting that during active infection, EBER1-mediated TLR3 stimulation is responsible for immune activation by EBV. TLR3 is predominantly expressed on DCs (Doyle et al., 2003; Akira and Takeda, 2004); circulating EBER1 could induce the activation of DCs and subsequent T cell activation, leading to the systemic production of proinflammatory cytokines. EBER1-mediated immune response would be needed for host defense, therefore IM, which is characterized as a CTL response against polyclonal proliferation of EBV-infected B cells usually follows a self-limited course. In EBV-HLH, EBV-infected cells are mainly $CD8^+$ T cells, whereas $CD4^+$ T or NK cells are infected in CAEBV (Kasahara et al., 2001). Given that $CD8^+$ T cells and NK cells express TLR3 and are activated by TLR3 signals (Schmidt et al., 2004; Tabiasco et al., 2006), TLR3-expressing T cells and NK cells could be activated by EBER1 through TLR3 and produce proinflammatory cytokines. Our findings suggest that immunopathologic diseases that are caused by active EBV infections could be attributed to TLR3-mediated cytokinemia

Published August 31, 2009

by EBER1, and that circulating EBER1 could be a potential target for therapeutic agents. Because it has been reported that plasmacytoid DCs are involved in anti-EBV immunity by the secretion of IFN and T cell activation through TLR9 pathways (Lim et al., 2007), TLR3 would collaborate with TLR9 during primary EBV infection.

Recent studies have demonstrated that activation of TLR3 by viral dsRNA contributes to viral pathogenesis. For example, TLR3-mediated inflammatory responses by viral dsRNA contribute to the development of lethal encephalitis by facilitating virus entry into the brain during West Nile virus infection (Wang et al., 2004). Rotavirus genomic dsRNA induces severe injury in the small intestine of mice in a TLR3-dependent manner (Zhou et al., 2007). These findings, along with ours, suggest that activation of TLR3 induces not only protective effects against viral infection but also effects that contribute to viral pathogenesis.

It was reported that EBER1 mostly binds to L22 (Toczyski and Steitz, 1993). Therefore, if EBER1 is released because of cell death, it would be released with Flag-L22 rather than other Flag-tagged proteins from the cell, in which those proteins are equally expressed. However, the majority of the EBER1 that was released from the cells existed in a complex with Flag-La, whereas other EBER-binding proteins, such as PKR and L22 were faintly detected. This led us to hypothesize that EBER1 is released from the cells by active secretion of La. Because La has been reported to be secreted as an exosome (Kapsogeorgou et al., 2005), EBER1 might also be secreted in this manner by binding to La. Alternatively, if La is more stable than L22 in extracellular state, EBER1 released by cell death could be strongly detected with La. Interestingly, we also demonstrated that EBER1 stimulates TLR3 in complexes with La protein. Further study is needed to clarify how the EBER1–protein complex is recognized by TLR3 and the mechanism of EBER1 release.

In contrast to EBER1, EBER2 was faintly detected in the culture supernatants of EBV-infected cells or in sera from patients with active EBV infections. EBER2 has a shorter half-life than EBER1, which may account for the preferential detection of EBER1 in our experiments (Clarke et al., 1992).

MATERIALS AND METHODS

Cell culture and reagents. LCLs, the EBV-positive Burkitt's lymphoma cell lines Akata+ (Takada, 1984) and Mutu+ (Gregory et al., 1990), and the EBV-negative cell lines Akata− (Shimizu et al., 1994) and Mutu− (Nanbo et al., 2002) were cultured in RPMI 1640 media (Sigma-Aldrich) supplemented with 10% FBS (Invitrogen) and antibiotics. Akata− cells that had been reinfected with recombinant EBER-positive EBV (Akata/EBER$^+$EBV; Shimizu et al., 1996) or EBER-knockout EBV (Akata/EBER$^-$EBV; Yajima et al., 2005) were cultured in RPMI 1640 media containing 700 μg/ml G418 (Sigma-Aldrich). EBV-infected (EBV+) and neomycin-resistant gene transfected (EBV−) NU-GC-3 cells and EBER-positive EBV or EBER-knockout EBV-infected AGS cells were cultured in Dulbecco's modified Eagle's medium (Sigma-Aldrich) supplemented with 10% FBS, antibiotics, and 500 μg/ml G418. The anti-Flag antibody and mouse IgG1 were purchased from Sigma-Aldrich. The anti-TLR3 antibody was obtained from eBioscience, and the anti-phospho IRF3 antibody, anti-IRF3 antibody, and anti-phospho p65 antibody were obtained from Cell Signaling Technology. poly(I:C) and polymyxin B were purchased from EMD. Anti-CD83 antibody and anti-CD86 antibody were obtained from Beckman Coulter and Ancell Co., respectively. Human recombinant GM-CSF and IL-4 were purchased from PeproTech.

RNA extraction and RT-PCR. Total RNA was extracted using Trizol reagent (Invitrogen) and was treated with DNaseI (Invitrogen). To analyze the release of EBER, RNA was extracted from 1 ml culture media or 100 μl serum and plasma. Reverse transcription was performed using SuperScript II reverse transcription (Invitrogen) and oligo-dT primer (Promega) or sequence-specific primers for EBER1 and EBER2. The sequence of the primers used for PCR was as follows. EBER1 (5′-AGGACCTACGCTGCCCTAGA-3′, 5′-AAAACATGCGGACCAGC-3′), EBER2 (5′-AGGGACAGCCGTTGCCCTAGTGGTTTCGGA-3′, 5′-AAAACAGCGGACAAGCCGAATACC-3′), TLR3 (5′-TCACTTGCTCATTCTCCCTT-3′, 5′-GACCTCTCCATTCCTGGC-3′), IFN−β (5′-GATTCATCGAGCACTGGCTGG-3′, 5′-CTTCAGGTAATGCAGAATCC-3′), IFN-γ (5′-CAGGTCATTCAGATGTAGCG-3′, 5′-GCTTTTCGAAGTCATCTCG-3′), TNF (5′-CTTCTGCCTGCTGCACTTTGGA-3′, 5′-TCCCAAAGTAGACCTGCCCAGA-3′), and GAPDH (5′-GCCTCCTGCACCACCAACTG-3′, 5′-CGACGCCTGCTTCACCACCTTCT-3′).

Quantification of EBER1. EBER1 was prepared by in vitro transcription as previously described (Samanta et al., 2006). Serial dilutions of EBER1 (0.1 ng/ml to 1.0 μg/ml) were made in culture media and total RNA was extracted and used for real-time PCR using the LightCycler system (Roche). These results were used as a standard for measuring the amount of EBER1 in culture supernatant.

Analysis of TLR3 activation. In vitro–synthesized EBER1 or poly(I:C) and RNAs that had been prepared from culture supernatants or human sera were mixed with Lipofectamine 2000 (Invitrogen) for 15 min in Opti-MEM (Invitrogen) before being used to stimulate the cells. The reagents were incubated in the tissue culture medium for 1 h before being removed by washing. To neutralize TLR3, cells were pretreated with an anti-TLR3 antibody (40 μg/ml) for 30 min at 37°C. The antibody was then removed before the TLR3 stimulation.

Measurement of cytokine production. Cell culture supernatants were collected and analyzed for IFN-β and IL-12 p40 production using a human IFN-β ELISA kit (PBL Biomedical Laboratories) or OptEIA human IL-12 (p40) ELISA kit (BD) according to the manufacturer's protocol.

Immunoblotting. Cells were lysed with 1% NP-40 lysis buffer and the cell lysates were subjected to SDS-PAGE and subsequent electrotransfer onto nitrocellulose membranes. The membranes were blocked with 5% bovine serum albumin (Sigma-Aldrich) or nonfat milk in TBS containing 0.05% Tween 20, and were subsequently treated with the primary antibodies for phospho-IRF3, IRF-3, phospho-p65, and the Flag tag.

Analysis of EBER-protein interactions by coimmunoprecipitation. Mutu cells (2×10^6) were transfected with Flag-La, Flag-L22, and Flag-PKR expression plasmids by electroporation. After 48 h, 1 ml culture supernatant was harvested and incubated with 3.5 μg anti-Flag mouse monoclonal antibody for 14 h at 4°C. After the addition of 50 μl of protein G–Sepharose (GE Healthcare), mixtures were incubated at 4°C for 3 h. Sepharose beads were pelleted and washed twice with lysis buffer (50 mM Tris-HCl, pH 7.4, 150 mM NaCl, 1% Nonidet P-40, 0.5% deoxycholate, and 20% protease/inhibitor) and three times with wash buffer (50 mM Tris-HCl, pH 7.4, 200 mM NaCl, 0.1% Nonidet P-40, 0.05% deoxycholate, 10% protease/inhibitor mix, 100 units/ml RNasin, 0.4% vanadyl ribonucleoside complex, and 1 mM dithiothreitol) by end-over-end rotation for 10 min. Pellets were dissolved in SDS loading buffer and subjected to immunoblotting. For RNA extraction, pellets were dissolved in 100 μl of lysis buffer and digested with 30 μg of proteinase K for 30 min at 50°C with the addition of 0.1% SDS,

before being dissolved in Trizol reagent. Extracted RNA was analyzed by RT-PCR for the expression of EBER1.

Flow cytometry. Cells were washed with FACS buffer (PBS containing 0.1% BSA, 0.1% NaN_3) and stained with anti-CD83 antibody (1 μg), anti-CD86 antibody (0.5 μg), or mouse IgG1 (1 μg) together with human IgG (10 μg) for 30 min at 4°C. After washing twice with FACS buffer, cells were incubated with FITC-labeled secondary antibody (American Qualex) for 30 min at 4°C, and then analyzed on a FACSCalibur (BD).

Preparation and stimulation of DCs. The institutional committee at Hokkaido University approved the use of human blood samples for this study. $CD14^+$ monocytes were isolated from human PBMC using a MACS system (Miltenyi Biotec). Immature DCs were generated from monocytes by culture for 6 d in RPMI 1640 medium supplemented with 10% heat-inactivated FCS (SAFC Biosciences) in the presence of 500 IU/ml recombinant human GM-CSF and 100 IU/ml recombinant human IL-4. Immature DCs (10^6 cells/ml) were treated with poly(I:C) (10 μg/ ml) or synthesized EBER1 (10 μg/ml) for 24 h. Both reagents were treated with polymyxin B (5 μg/ml) at 37°C for 1 h before stimulation.

TLR3 knockdown experiment. TLR3 stealth RNAi (Invitrogen) or stealth RNAi negative control (Invitrogen) was transfected using Lipofectamine RNAiMAX (Invitrogen) according to the manufacturer's protocol. Successful transfection was confirmed using the BLOCK-iT Alexa Fluor Red Fluorescent Oligo (Invitrogen). Monocytes were cultured for 4 d before being transfected (10^6 cells/well, 24 well plate) on day 4 and again on day 5 with 70 nM siRNA. On day 6 (48 h after the first transfection), cells were used for stimulation. AGS cells (10^5 cells/well, 24-well plate) were transfected with 10 nM siRNAs and used for stimulation after 48 h.

Mixed lymphocyte reaction (MLR) assay. After 24 h stimulation with poly(I:C) or EBER1, DCs were treated with 50 μg/ml mitomycin C (MMC). Allo-PBMC were isolated by Histopaque density gradient separation of blood collected from healthy donors. Serial dilutions (10^4 to 10^3 cells/well) of MMC-treated DCs were cultured in triplicate with 10^5 PBMCs in 96-well round-bottom plates for 3 d, and PBMC proliferation was measured using CellTiter 96 nonradioactive cell proliferation assay kit (Promega).

We thank Y. Ando for technical assistance.

This work was supported by grants-in-aid from the Ministry of Education, Science, Sports, Culture and Technology, Japan (D. Iwakiri and K. Takada) and by the Takeda Science Foundation and the Akiyama Foundation (D. Iwakiri).

The authors have no conflicting financial interests.

Submitted: 7 August 2008
Accepted: 10 August 2009

REFERENCES

Akira, S., and K. Takeda. 2004. Toll-like receptor signalling. *Nat. Rev. Immunol.* 4:499–511. doi:10.1038/nri1391

Akiyama, S., H. Amo, T. Watanabe, M. Matsuyama, J. Sakamoto, M. Imaizumi, H. Ichihashi, T. Kondo, and H. Takagi. 1988. Characteristics of three human gastric cancer cell lines, NU-GC-2, NU-GC-3 and NU-GC-4. *Jpn. J. Surg.* 18:438–446. doi:10.1007/BF02471470

Clarke, P.A., M. Schwemmle, J. Schickinger, K. Hilse, and M.J. Clemens. 1991. Binding of Epstein-Barr virus small RNA EBER-1 to the double-stranded RNA-activated protein kinase DAI. *Nucleic Acids Res.* 19:243–248. doi:10.1093/nar/19.2.243

Clarke, P.A., N.A. Sharp, and M.J. Clemens. 1992. Expression of genes for the Epstein-Barr virus small RNAs EBER-1 and EBER-2 in Daudi Burkitt's lymphoma cells: effects of interferon treatment. *J. Gen. Virol.* 73:3169–3175. doi:10.1099/0022-1317-73-12-3169

Doyle, S.E., R. O'Connell, S.A. Vaidya, E.K. Chow, K. Yee, and G. Cheng. 2003. Toll-like receptor 3 mediates a more potent antiviral response than Toll-like receptor 4. *J. Immunol.* 170:3565–3571.

Gregory, C.D., M. Rowe, and A.B. Rickinson. 1990. Different Epstein-Barr virus-B cell interactions in phenotypically distinct clones of a Burkitt's lymphoma cell line. *J. Gen. Virol.* 71:1481–1495. doi:10.1099/0022-1317-71-7-1481

Imai, S., J. Nishikawa, and K. Takada. 1998. Cell-to-cell contact as an efficient mode of Epstein-Barr virus infection of diverse human epithelial cells. *J. Virol.* 72:4371–4378.

Kapsogeorgou, E.K., R.F. Abu-Helu, H.M. Moutsopoulos, and M.N. Manoussakis. 2005. Salivary gland epithelial cell exosomes: a source of autoantigenic ribonucleoproteins. *Arthritis Rheum.* 52:1517–1521. doi:10.1002/art.21005

Kasahara, Y., A. Yachie, K. Takei, C. Kanegane, K. Okada, K. Ohta, H. Seki, N. Igarashi, K. Maruhashi, K. Katayama, et al. 2001. Differential cellular targets of Epstein-Barr virus (EBV) infection between acute EBV-associated hemophagocytic lymphohistiocytosis and chronic active EBV infection. *Blood.* 98:1882–1888. doi:10.1182/blood.V98.6.1882

Kikuta, H., Y. Sakiyama, S. Matsumoto, T. Oh-Ishi, T. Nakano, T. Nagashima, T. Oka, T. Hironaka, and K. Hirai. 1993. Fatal Epstein-Barr virus-associated hemophagocytic syndrome. *Blood.* 82:3259–3264.

Lerner, M.R., N.C. Andrews, G. Miller, and J.A. Steitz. 1981. Two small RNAs encoded by Epstein-Barr virus and complexed with protein are precipitated by antibodies from patients with systemic lupus erythematosus. *Proc. Natl. Acad. Sci. USA.* 78:805–809. doi:10.1073/pnas.78.2.805

Lim, W.H., S. Kireta, G.R. Russ, and P.T. Coates. 2007. Human plasmacytoid dendritic cells regulate immune responses to Epstein-Barr virus (EBV) infection and delay EBV-related mortality in humanized NOD-SCID mice. *Blood.* 109:1043–1050. doi:10.1182/blood-2005-12-024802

Matsumoto, M., S. Kikkawa, M. Kohase, K. Miyake, and T. Seya. 2002. Establishment of a monoclonal antibody against human Toll-like receptor 3 that blocks double-stranded RNA-mediated signaling. *Biochem. Biophys. Res. Commun.* 293:1364–1369. doi:10.1016/S0006-291X(02)00380-7

Nanbo, A., K. Inoue, K. Adachi-Takasawa, and K. Takada. 2002. Epstein-Barr virus RNA confers resistance to interferon-α-induced apoptosis in Burkitt's lymphoma. *EMBO J.* 21:954–965. doi:10.1093/emboj/21.5.954

Rickinson, A.B., and E. Kieff. 2001. Epstein-Barr virus. *In* Fields Virology. Fourth edition. B.N. Fields, D.M. Knipe, and P.M. Howley, editors. Lippincott Williams & Wilkins, Philadelphia. 2575–2627.

Rosa, M.D., E. Gottlieb, M.R. Lerner, and J.A. Steitz. 1981. Striking similarities are exhibited by two small Epstein-Barr virus-encoded ribonucleic acids and the adenovirus-associated ribonucleic acids VAI and VAII. *Mol. Cell. Biol.* 1:785–796.

Rymo, L. 1979. Identification of transcribed regions of Epstein-Barr virus DNA in Burkitt lymphoma-derived cells. *J. Virol.* 32:8–18.

Samanta, M., D. Iwakiri, T. Kanda, T. Imaizumi, and K. Takada. 2006. EB virus-encoded RNAs are recognized by RIG-I and activate signaling to induce type I IFN. *EMBO J.* 25:4207–4214. doi:10.1038/sj.emboj.7601314

Schmidt, K.N., B. Leung, M. Kwong, K.A. Zarember, S. Satyal, T.A. Navas, F. Wang, and P.J. Godowski. 2004. APC-independent activation of NK cells by the Toll-like receptor 3 agonist double-stranded RNA. *J. Immunol.* 172:138–143.

Shimizu, N., A. Tanabe-Tochikura, Y. Kuroiwa, and K. Takada. 1994. Isolation of Epstein-Barr virus (EBV)-negative cell clones from the EBV-positive Burkitt's lymphoma (BL) line Akata: malignant phenotypes of BL cells are dependent on EBV. *J. Virol.* 68:6069–6073.

Shimizu, N., H. Yoshiyama, and K. Takada. 1996. Clonal propagation of Epstein-Barr virus (EBV) recombinants in EBV-negative Akata cells. *J. Virol.* 70:7260–7263.

Tabiasco, J., E. Devêvre, N. Rufer, B. Salaun, J.C. Cerottini, D. Speiser, and P. Romero. 2006. Human effector CD8+ T lymphocytes express TLR3 as a functional coreceptor. *J. Immunol.* 177:8708–8713.

Takada, K. 1984. Cross-linking of cell surface immunoglobulins induces Epstein-Barr virus in Burkitt lymphoma lines. *Int. J. Cancer.* 33:27–32. doi:10.1002/ijc.2910330106

Toczyski, D.P., and J.A. Steitz. 1993. The cellular RNA-binding protein EAP recognizes a conserved stem-loop in the Epstein-Barr virus small RNA EBER 1. *Mol. Cell. Biol.* 13:703–710.

Published August 31, 2009

Toczyski, D.P., A.G. Matera, D.C. Ward, and J.A. Steitz. 1994. The Epstein-Barr virus (EBV) small RNA EBER1 binds and relocalizes ribosomal protein L22 in EBV-infected human B lymphocytes. *Proc. Natl. Acad. Sci. USA.* 91:3463–3467. doi:10.1073/pnas.91.8.3463

Wang, T., T. Town, L. Alexopoulou, J.F. Anderson, E. Fikrig, and R.A. Flavell. 2004. Toll-like receptor 3 mediates West Nile virus entry into the brain causing lethal encephalitis. *Nat. Med.* 10:1366–1373. doi:10.1038/nm1140

Yajima, M., T. Kanda, and K. Takada. 2005. Critical role of Epstein-Barr Virus (EBV)-encoded RNA in efficient EBV-induced B-lymphocyte growth transformation. *J. Virol.* 79:4298–4307. doi:10.1128/JVI.79.7.4298-4307.2005

Zhou, R., H. Wei, R. Sun, and Z. Tian. 2007. Recognition of double-stranded RNA by TLR3 induces severe small intestinal injury in mice. *J. Immunol.* 178:4548–4556.